NASA CR-72296

FINAL REPORT

DEVELOPMENT OF

CADMIUM SULFIDE PHOTOVOLTAIC FILM CELLS

Prepared For

NATIONAL AERONAUTICS AND SPACE ADMINISTRATION

OCTOBER 1967

CONTRACT NAS3-8515

THE HARSHAW CHEMICAL CO.

NOTICE

This report was prepared as an account of Government sponsored work. Neither the United States, nor the National Aeronautics and Space Administration (NASA), nor any person acting on behalf of NASA:

A). Makes any warranty or representation, expressed or implied, with respect to the accuracy, completeness, or usefulness of the information contained in this report, or that the use of any information, apparatus, method, or process disclosed in this report may not infringe privately owned rights; or

B). Assumes any liabilities with respect to the use of, or for damages resulting from the use of any information, apparatus, method or process disclosed in this report.

As used above, "person acting on behalf of NASA" includes any employee or contractor of NASA, or employee of such contractor, to the extent that such employee or contractor of NASA, or employee of such contractor prepares, disseminates, or provides access to, any information pursuant to his employment of contract with NASA, or his employment with such contractor.

Requests for copies of this report should be referred to:

National Aeronautics and Space Administration
Office of Scientific and Technical Information
Attention: AFSS-A
Washington, D. C. 20546

TABLE OF CONTENTS

DEVELOPMENT OF CADMIUM SULFIDE PHOTOVOLTAIC FILM CELL

By

J. C. Schaefer, J. Evans, and T. A. Griffin

ABSTRACT

Control of the carrier concentration in the CdS film has provided improved yields. Voltages up to 0.55 volts and cell conversion efficiencies up to 7.1% were reported with typical cell efficiencies ranging from 4.0 to 5.4%. The correlation between cell open circuit voltage and carrier concentration of the film has been demonstrated.

Summary

The scope of this program required studies directed towards improvement in the reproducibility of high efficiency cells and the elimination of storage degradation of CdS thin film solar cells on molybdenum substrates. The objectives established for the contract were (1) operation of a pilot line to investigate iinprovements and to determine yields, and (2) to increase cell efficiency by contrclled doping of the CdS film. It was found that controlled carrier concentration affected an efficiency increase and produced an increase in yield.

Studies have shown a correlation between film carrier concentration and final cell open circuit voltage. Carrier concentrations studied ranged from 10^{16} to 10^{19} carriers per cm3. Cell open circuit voltages ranged from 0.34 to 0.54 volts.

CdS polycrystalline films were doped with group IB acceptor atoms copper, silver, and gold, and Group III B donor atoms cadmium, indium and gallium. It was not possible to detect the dopants in the film when the starting material contained 0.01, 0.001 and 0.0001 atomic percent impurities specified. A large excess of dopant was required in the initial charge in the boat to obtain detectable amounts in the film.

Acid etching of the CdS film before barrier formation was found to be essential. Approximately 1 micron (0.5 milligrams per cm^2) must be removed from a 25 micron thick evaporated CdS film. Although sulfuric acid provided the most consistent results for the major portion of study, after process changes were made hydrochloric acid yielded cells with the highest efficiencies.

The barrier formation was examined from the standpoint of aqueous and non-aqueous solvent baths. Organic baths produced cells of slightly higher open circuit voltage but lower current density than those from the aqueous baths.

Conversion from the mylar-nylon type of encapsulation to the mylar-epoxy and the Kapton-epoxy types necessitated a change in time and temperature for lamination. The heat applied to the cell affected the junction and required continual reevalua-

tion of cell processing. The epoxy type package does provide a more stable cell.

Both the electroplated and the thermo-compression type grids were investigated. Using a non-cyanide gold plating bath, electroplated grid cells were fabricated with efficiencies up to 5.3% on nominal 3" x 3" areas. As directed by NASA, the electroplated grid process was discontinued in the seventh month.

It was demonstrated that a CdS thin film cell can be griddcd with as few as 20 lines per inch. This grid can collect the current efficiently for those cells having a low barrier sheet resistance.

Maximum cell efficiencies are reported as 7.1% for a 3.7 cm^2 cells and 5.4% for the 44 cm^2 units (at a temperature of 25°C and simulating conditions of air mass 1 100 mw/cm^2 sunlight). The light source used for these tests was calibrated against standards provided by NASA-Lewis Research Center. The standards were calibrated at high altitude and terrestrial sun light, and were cross referenced in the Le.R.C. laboratory.

LIST OF FIGURES

LIST OF TABLES

Introduction

This report describes the research and development performed on a thin film energy conversion device as a follow-on effort to contract NAS3-7631. .The device converts solar energy to electrical energy by means of a junction between cadmium sulfide and copper sulfide. The completed device is thin, flexible and lightweight. The contents of the report have been arranged in a sequence corresponding to the order of fabrication. A flow diagram has been included.

The thin film cadmium sulfide solar cell has been developed sufficiently to become attractive as a space power source. The problems of reproducibility in the production of high efficiency cells and the retention of such efficiency over a long storage period were to be studied.

Two objectives were established as a means of studying the above problems. A laboratory assembly line for cell fabrication was to be used to investigate improvements and to increase yields. The second objective was to affect an increase in cell efficiency by doping the cadmium sulfide.

This report discusses the methods used and interprets data obtained in reaching these objectives.

Each processing step in the assembly line was evaluated and reevaluated when indicated. Prior to the present work a large variation in film properties was evident. One of these is the carrier concentration of the film. Pressure control during evaporation has aided in regulating the carrier concentration. As a result, the correlation of carrier concentration to cell open circuit voltage has been demonstrated.

CdS polycrystalline films were doped with group IB acceptor atoms copper, silver, and gold, and Group III B donor atoms, cadium, indium and gallium. It was not possible to detect the dopants in the film when the starting material contained 0.01, 0.001 and 0.0001 atomic percent impurities. A large excess of dopant was required in the starting material to realize detectable amounts

in the films. These cells were processed in the standard manner. The majority of cells had linear I-V characteristics, the remainder having very poor diode characteristics with low current output and an open circuit voltage less than 0.35 volts. With such poor characteristics it was not possible to obtain meaningful capacitance measurements because of the very large dissipation factors. Spectral response measurements were made whenever possible but showed no significant variation from those obtained for undoped CdS films with the same carrier concentrations. The ceils made from the undoped CdS films, which were produced from the same evaporator, had an average efficiency of between 4 and 5 percent. High efficiency cells were never made from those films with carrier concentrations less than 3×10^{17} per cm^3. Typical spectral responses for the undoped CdS cells are shown. These films all had resistivities of the order of 1 ohm cm. The cells produced had capacitances of the order of 20 millimicrofarads per cm^2.

The effect of etching the CdS films was studied extensively. Initially experiments showed concentrated sulfuric acid to be the preferred etchant. After changes in cell fabrication techniques, a repetition of the above experiments indicated that dilute HCl was the better etchant. It gave higher current densities.

The barrier formation has been established as an exchange reaction between copper (ous) and cadmium resulting in the formation of a cuprous sulfide layer at the surface of the etched cadmium sulfide. The amount and quality of cuprous sulfide formed is a function of immersion time, temperature, and composition of the bath. A saturated cuprous chloride bath is satisfactory but its useable life is about three hours. A complex copper bath has been developed with a lifetime of about three weeks. Immersion times are always less than one minute at elevated temperatures.

Experiments with organic solvents and molten salts were conducted in an attempt to reduce the amount of ambient water and oxygen during chemi-plating. Bath temperatures were higher for the molten salts and reaction rates were so rapid that most of the CdS was converted to Cu_2S. The use of organic solvents

permitted bath temperatures up to 160°C. Salt concentrations up to 1500 grams per liter were possible for the organic baths, compared to 1.5 grams per liter in water. This made available an excess supply of copper with a greatly improved bath stability.

Heat must be applied to the CdS-Cu_2S unit to form a junction. The heat is obtained from (1) the barrier bath (90°C for 5 seconds), (2) subsequent heat treatment (250°C for 2 minutes), and (3) lamination (190°C for 30 minutes). It has been found that the heat treatment at 250°C should be tailored to a given cell with the time range of 0 to 2 minutes. A photovoltaic response before lamination is important in obtaining a high efficiency cell.

Film Formation by Close Space Vapor Transport

The formation of CdS films by evaporation is of such a nature that more controllable methods are desirable. Close space vapor transport [1] was chosen.

Although the details of the method varied during the investigation, certain essential features remained the same. All film forming operations were performed in a vacuum bell jar system. The cadmium sulfide charge was distributed evenly across a flat pan. The substrate was positioned a short distance above the pan. Pressures of operation (gauge) were held in the range of 1 to 10 microns. The close proximity of the substrate to the boat literally formed a closed box. The pressure in this system was considerably higher than for evaporation.

Boat materials selected for examination were tantalum and quartz. The tantalum was attacked slowly producing a layer of powder between the tantalum and the residual CdS. This also changed the transport rate. The combination of a quartz boat positioned on a tantalum heating strip was found to be satisfactory. A thermocouple was attached below the heating strip. A similar sensor was positioned above the substrate.

A heater was placed above the substrate to supply heat as needed.

Substrate materials investigated were molybdenum, copper, 1010 steel, invar, copper-clad molybdenum, brass, chromium-plated zirconium, and titanium. At the temperatures required for transport, only molybdenum and titanium retained suitable properties. Copper and copper-coated molybdenum deteriorated because of conversion to copper sulfide. The CdS deposited on the steel and invar lacked adhesion, while that deposited on the chromium-plated zirconium adhered to some extent. Sand-blasted molybdenum was the most suitable. Acid etched molybdenum was not suitable for film thicknesses greater than 0.7 mil, [17μ].

An excess of cadmium in the film was not apparent as in the case of evaporation. Dopants had to be mixed with the CdS charge to obtain lower resistivity films. Control and reproducibility were considered to be good. Table I shows typical results which are plotted in Figure 2.

Table I

Data on Dopant Conc. and Resistivity - Vapor Transport

Film Sample No.	Dopant in Charge	Film Thickness	Film Resistivity
V 132	0 mol %	25μ	$4.3 \times 10^{+4}$ ohm-cm
V 247	1.7×10^{-2}	29	3.8×10^{3}
V 266	3.0×10^{-2}	12	1.9×10^{2}
V 212	5.0×10^{-2}	22	3.8
V 263	5.0×10^{-2}	25	3.5

The general procedure was to evacuate and refill with argon several times and to use a titanium strip as a getter. A gauge pressure between 1 and 10 microns was maintained during each run.

The boat temperature ranged from 600 to 900°C. The usual temperature range was 830 to 850°C. A temperature differential

of 50 to 150°C was always maintained between boat and substrate as opposed to a 800 to 900°C differnece for evaporation.

A phenomenon which had originally been assumed to be spatter on the surface of the films was discovered to be whisker growth of CdS. The growth was such that the whiskers would flex and wave with changes in air current across the surface. Figure No. 3 is included to illustrate the individual whiskers. They appear to have had a molten tip during growth which solidified on cooling.

Cells made from these films were not good. Better electrical characteristics were noted for films from which the whiskers had been removed. There are indications that in evaporated films those with small crystalline patterns produced cells superior to those from films displaying large crystalline patterns.

Cell quality of vapor transport films never equalled that obtained from normal evaporation conditions. It may be that the barrier formation procedures best suited for evaporated films are not suited for the vapor transport films. A continuation of this work would have to take this into consideration.

Film Dopant Study:

Discussion

This work was a study of the effect of doping the CdS films as a possible method of increasing cell efficiency.

The first approach was the doping of the CdS powder to the required level and then evaporating from a single source. Each boat required 15 grams of CdS with 100, 10 and 1 ppm dopant respectively. Batches of 200 grams were processed at a time. Initially, this amount of powder was doped to the level of 0.01 atomic percent and mixed thoroughly in a blender for several hours. Then 20 grams of this powder were mixed with a known weight of CdS to reduce the doping level to 0.001 atomic percent. This procedure was again repeated to attain the lowest doping level of 0.0001 atomic percent. Calculations of carrier concentration were made assuming that the composition of the evaporated film was that of powder charge and that all the dopant and only the dopant was

ionized. The values obtained were 2×10^{18}, 2×10^{17}, and 2×10^{16} carriers per cm^3 respectively. A comparison between these calculated values and those obtained from Hall co-efficient data is shown in Table 11. The expected correlation between doping level and corresponding carrier concentration was not evident.

In the undoped CdS evaporated film, the carriers are due to the excess cadmium incorporated into the cadmium sulfide lattice. In order to see any effects due to dopant atoms, the concentration of the excess Cd in the lattice would have to be reduced to a minimum of 10^{16} carriers per cm^3. Then, for example, the carriers provided by the dopant atoms (2×10^{16} per cm^3 at the lowest doping level) would be in the majority. Therefore, a method had to be found to produce undoped CdS films of a controlled low carrier concentration.

In order to achieve this, a thorough investigation had to be made of the parameters in the evaporation process that play a dominant role in the properties of the final film. The variables investigated were rate of evaporation and substrate temperature. These two factors govern the rate of deposition. The carrier concentration was then plotted versus rate of deposition. The graph indicated that a low rate would produce a low carrier concentration. The evaporating system was then completely modified. Cooling coils were incorporated on the base plate and at the feedthroughs for the power terminals to dissipate the heat produced during the long runs. Some evaporations required 24 hours. The results obtained both before and after this change are shown in Figure 4. Those obtained after the modification show a great deal of scatter indicating that rate of deposition alone was not the only factor governing the carrier concentration, Films with the required low carrier concentration were not obtained and the disadvantages of running very long evaporations were numerous.

Table II

Doped Samples

Sample	Doping Level Atomic Percent	Calculated Carriers/cc	Hall Measurements Carriers/cc
AI-010-1			6.45 x 10^{18}
Al-010-2	.01 Al %	2 x 10^{18}	Hall sample peeled off Substrate
Al-010-3			3.9 x 10^{18}
Al-001-1			1.5 x 10^{18}
Al-001-2	.001 Al %	2 x 10^{17}	6.25 x 10^{17}
Al-001-3			6.63 x 10^{17}
Al-001-1			7.15 x 10^{17}
Al-001-2	.0001 Al %	2 x 10^{16}	6.25 x 1017
Al-001-3			2.01 x 1018
In-010-1			1.37 x 10^{18}
In-010-2	.01 In %	2 x 10^{18}	2.51 x 10^{18}
In-010-3			5.45 x 10^{18}
			7.45 x 10^{18}
In-001-1			2.4 x 10^{18}
In-001-2	.001 In %	2 x 10^{17}	2.23 x 10^{18}
In-001-3			1.66 x 10^{18}
In-0001-1			9.26 x 1017
In-0001-2	.0001 In %	2 x 10^{16}	1.01 x 10^{18}
In-0001-3			1.01 x 1018

A new approach was tried utilizing techniques similar to those of vapor transport. In this case, the substrate temperature was 200°C, the boat temperature was 700-800°C and the separation between the source and substrate was 4 cms. A diagram is shown in Figure 5. Initially it was difficult to produce thick enough films. This was caused by reevaporation from the substrate in places that had received excessive heat radiated from the boat. This was overcome by completely covering the CdS powder in the boat with a thin layer of ceramic fiber, giving some protection and enabling much more uniform films to be produced. This also eliminated the ejection of CdS grains from the boat. The adhesion between the CdS film and molybdenum substrate was improved by sandblasting the substrate, but the films did not endure subsequent processing in all cases.

During this time, a new technique had to be introduced to measure low values of carrier concentration. The carriers in the evaporated film have a low mobility. When this is combined with the high resistivity inherent in films with carrier concentrations between 1×10^{16} and 1×10^{17} carriers per cm^3, operating conditions are such as to approach the limit of resolution of the signal in Hall voltage measurements. Measurements of the Seebeck voltage and temperature drop across the length of the sample permitted the determination of low carrier concentration from a calibration curve. This method has the added advantage of being simple.

The close space method gave low carrier concentration CdS films. Work then continued on doping films. In_2S_3, $InCl_3$ and $AlCl_3$ were used as the dopants, but with no increase in carrier concentration. It was suspected for In_2S_3 that this was due to low vapor pressure, therefore $InCl_3$ was substituted. No change was noted. Spectrographic analysis then showed that the composition of the film was not that of the powder. In fact the highest doping level of 100 ppm in the powder gave less than 1 ppm dopant in the final film.

The $AlCl_3$ gave poor results. At this point it appeared likely that a chemical reaction was occurring in the boat converting the chloride to the sulphide, which has an extremely

low vapor pressure. At a boat temperature of about 800°C aluminum sulphide could not be evaporated.

It was possible to raise the carrier concentration in the film by adding a large excess of dopant, that is for example, 5 mgms impurity to 15 grams CdS charge used in the boat. Many of these doped films were processed. They were characterized by a low open circuit voltage and a high series resistance, the latter probably being caused by poor adherence between film and substrate. Because of very poor dark curves and low fill factor in the light curves, it was difficult to ensure meaningful data from capacitance and spectral response measurements.

Because films produced by this close spaced method of evaporation resulted in poor cells, the standard evaporation procedure was resumed. One parameter that had not previously been correlated with film properties was the pressure within the bell jar. There is difficulty in obtaining an absolute measurement of pressure between source and substrate, because it is not feasible to operate a gauge for any length of time in an atmosphere where it would become coated with CdS. Monitoring the pressure at some external point in the line did show that a high pressure within the bell jar, in the range 10^{-4}-10^{-5} torr could give films of carrier concentration within the range 10^{16} - 10^{-17} per cm^3. A pyrex chimney introduced to enclose the space between source and substrate-ensures more control over the atmosphere in which the film grows. (Figure 6.) This also reduces the possibility of contamination from impurities remaining on parts within the bell jar. The chimney was cleaned after each evaporation.

Films produced using the chimney had low resistivities of the order of 1 ohm cm. Values of 10 - 100 ohm cm were characteristic of films produced under the standard evaporation conditions with the same carrier concentration. It became apparent that there were certain minimum requirements for the system from which films with reproducible, controlled characteristics may be produced. The tantalum boats "age" rapidly and are essentially different for each subsequent evaporation.

With the present design it is also difficult to position a thermocouple such that it will remain free from corrosion and survive the evaporation. The tantalum boat should be superseded by a quartz boat of different design, [2] in which the thermocouple is fully protected, permitting the boat temperature to be monitored throughout the run. This new boat combined with the pyrex enclosure and uniformly heated substrate should make possible the production of films with more consistent qualities.

Experiments were conducted to incorporate Group I-B acceptor impurities of copper, silver, and gold into the evaporated film. As for the donor elements, an excess of acceptor dopant had to be mixed in with the CdS charge in order to detect any in the film. Those films produced in the three cases had high values of carrier concentration of approximately 1×10^{19} per cm^3. This was a factor of 10 greater than that obtained for undoped CdS film evaporated under the same conditions and is the reverse of what might have been expected. It may be that the majority of the dopant was migrating to the grain boundaries and not being incorporated in the film as an acceptor. This, of course, raises the question as to whether or not the Group III donor impurities might also have acted in a like manner.

There are two considerations which place doubt on this interpretation. First, dopants are normally incorporated into a crystal lattice with ease. Secondly, the surface of the doped sample, on which the measurements were made, was leached in cyanide to remove the dopant. The carrier concentration and resistivity were remeasured but showed no significant change. An explanation of this might be that only the surface dopant atoms were removed allowing any change to go undetected because of too low a sensitivity in the measurement. However, the results are puzzling and must await further experimentation.

Conclusions

When undoped CdS films are produced by the standard evaporation procedure the carrier concentrations vary between the limits of 2×10^{17} and 2×10^{18} per cm^3. This is due to native

defects in the film, that is, excess Cd incorporated into the CdS lattice. In order to see the effect of dopant atoms the concentrations of these native defects should be reduced to 10^{16} per cm^3. The reason for this lower limit is that at the doping level of 0.0001 atomic percent the carriers contributed to the lattice would be 2×10^{16} per cm^3 and would be in the majority. Therefore, a major part of the time was devoted to the investigation of the parameters which played a dominant role in determining the carrier concentration of the pure evaporated CdS film. Methods described earlier were found to produce films with carrier concentrations ranging from 1×10^{16} to 5×10^{18} per cm^3. It was then possible in the case of indium and gallium to incorporate dopant atoms into the film, but the concentration was always less than that of the starting material. No success was achieved with aluminum.

The group IB acceptor atoms copper, silver, and gold were incorporated into the film. The Seebeck voltage measurements indicated an increase in carrier concentration rather than a decrease which would be expected on adding a p-type dopant to an n-type lattice. The results of making cells from doped films have not been encouraging. The majority had linear I-V characteristics. The remainder were very poor diodes having open circuit voltages less than 0.35 volts, with low current output.

Undoped CdS films with carrier concentrations varying over the range 2×10^{16} to 3×10^{18} per cm^3 were investigated. Only those in the range of 5×10^{17} and 3×10^{18} per cm^3 and having a resistivity in the order of 1 ohm-cm produced good cells. The efficiency values were consistently between 4 and 5 percent.

Typical spectral response curves of these particular cells are shown in Figures 7a and 7b. A comparfson of the two curves shows a difference in cell output with the first curve showing a greater overall response. The increase in response at 2.4 eV in Figure 7a indicates that part of the junction is in the CdS. The rapid decay of response above 2.5 eV in Figure 7b is not readily explainable in terms of a simple p-n junction model.

Surface Etching of CdS

The goal of this study was to determine how the etching of the CdS film affected cell efficiency.

The etchants used were: concentrated HCl; 1:1 HCl:H_2O, concentrated H_2SO_4; 1:1 H_2SO_4:H_2O; 40% HI; 48% HBr and concentrated HNO_3. The etching rates were obtained by immersing samples of CdS films into each of the above etchants for various time intervals. The mass change of the CdS film was plotted versus the time of immersion. A representative set of curves is shown in Figure 8.

The etching rates of 1:1 HCl:H_2O and 40% HI are linear with time. The etching rates of concentrated HCl, concentrated H_2SO_4 and 48% HBr follow a square root curve. This leads one to conclude that etching is diffusion limited in the latter case. This limitation could be attributed to the fact that the etchant is not in immediate contact with the CdS surface at all times during the etching process. In the case of concentrated H_2SO_4, where the etching rate is slower, this is more obvious. After a film was exposed to H_2SO_4 for a short time a thin milky coating formed on the surface. This layer obviously affected the etching rate. In order to achieve an immediate contact between the etchant and the surface the etchants were agitated. However, this did not make all rates linear. It only increased them slightly.

There are two possible explanations why the etching of the CdS surface prior to the formation of the barrier layer is beneficial. The etchants remove either any annealed thin layers of CdS from the surface, or the amorphous CdS which is deposited between the crystallites during the last phase of the evaporation. Consequently, the amount of CdS removed or the etching depth is of primary importance,

Having obtained the etching rates for all etchants investigated, the CdS films could be etched to a predetermined depth. Various amounts of CdS were removed ranging from 0.20 to 1.5 mgms per cm^2. Cells were made from all the samples. In general the values of open circuit voltage and short cir-

cuit current were comparable for all samples which had the same amount of CdS removed. However, in the 1.0 to 1.5 mgms per cm^2 range the open circuit voltage values were low and the shunt resistances were rather poor. These resulted in low efficiency cells. The poor shunt resistance values and the low values of open circuit voltage can be explained as follows. When as much as 1.0 mgm per cm^2 or more of CdS is removed, the etching along the grain boundaries of the crystallites was too deep. Then when the barrier layer was formed the distribution of copper sulfide was uneven. This resulted in a deeply penetrating layer of Cu_2S and poor I-V characteristics. Because of these observations it was concluded that 0.7 mgms per cm^2 of CdS is the permissible limit of the mass that can be removed and 0.3 to 0.5 mgms per cm^2 was optimum. The amount of copper sulfide formed per unit area on a uniformly etched CdS surface is independent of the amount of CdS removed. The time of immersion alone determines the amount of copper sulfide formed. A weight gain after plating was detected. This confirmed that there is indeed a double displacement reaction taking place. Two copper ions in the cuprous state are substituting for each displaced cadmium ion.

With the exception of H_2SO_4 and HNO_3, the other etchants did not leave any residues behind. The residue on the surface of the CdS after etching in H_2SO_4 can be adequately removed with distilled water. Etching with nitric acid was not examined thoroughly for two reasons. First, it attacks CdS violently and etches in a manner very difficult to control. Second, it leaves behind areas of amorphous sulfur.

For the initial portion of this study H_2SO_4 was the preferred etchant because the resulting cells were more stable. Cells made after HCl etching, while initially as good as those made after H_2SO_4 etching, were less stable. However, when the encapsulating material was changed from Mylar-Nylon to Mylar-Astrochemical cement, cells made using both H_2SO_4 and HCl etchants were stable. When a more efficient rinsing technique was employed after etching 1:1 HCl:H_2O was the preferred etchant since the resulting cells had higher current densities with higher efficiences. See Table 111.

TABLE III a

Film #323 - 1.3 mils thick - No dopant - 2.5 x 10^{17} carriers/cm^3 - etchant and time varied
Au plated Cu Grid

Film#	Etchant	Etch Time (sec)	Voc (Volts)	Isc (ma)	Pwr (mw)	Eff. (%)	Days after lamination
1	conc H_2SO_4	0	.41	26	5.0	1.35	5
2	conc H_2SO_4	0	.40	32	5.6	1.51	5
3	conc H_2SO_4	0	.43	34	8.8	2.38	5
Avg.			.41	31	6.5	1.75	
4	conc H_2SO_4	60	.43	36	9.5	2.57	5
5	conc H_2SO_4	60	.44	36	9.2	2.49	5
6	conc H_2SO_4	60	.37*	26*		<1.35*	5
Avg			.44	36	9 4	2.53	
7	conc H_2SO_4	80	.42	29	5.0	1.35	5
8	conc H_2SO_4	80	.37*	28*		<1.35*	5
9	conc H_2SO_4	80	.41	40	5.7	1.54	5
Avg.			.42	35	5.4	1.45	
H_2SO_4 Avg.			.42	34	7.1	1.91	
10	1:1 HCl	10	.47	37	11.0	2.97	5
11	1:1 HCl	10	.48	47	13.1	3.54	5
12	1:1 HCl	10	.47	40	10.8	2.92	5
Avg.			.47	41	11.6	3.14	
13	1:1 HCl	15	.47	47	13.6	3.68	5
14	1:1 HCl	15	.46	45	12.0	3.24	5
15	1:1 HCl	15	.45	47	12.0	3.24	5
Avg			.46	46	12.5	3.39	
16	1:1 HCl	20	.47	46	12.6	3.40	5
17	1:1 HCl	20	.47	48	12.5	3.38	5
18	1:1 HCl	20	.45	45	11.3	3.06	5
Avg.			.46	46	12.1	3.28	
HCl Avg.			.46	44	12.1	3.27	

Test Area: 3.7 cm^2

*Not included in averages

TABLE III b

Film #353 - 1.3 mils thick - In_2S_3 doped - 2 x 10^{18} carriers/cm^3 - etchant and time varied
Au plated Cu Grids

Film#	Etchant	Etch Time (Sec)	Voc (Volts)	Isc (mA)	Pwr (mw)	Eff (%)	Days after Lamination
1	concH_2SO_4	40	.41	40	8.2	2.22	6
10	concH_2SO_4	40	.43	37	10.1	2.73	6
11	concH_2SO_4	40	.42	39	10.0	2.71	6
Avg.			.42	39	9.5	2.59	6
2	concH_2SO_4	≤0	41	39	10 5	2 84	6
12	Dropped in bath						
13	concH_2SO_4	≤0	.37*	22*		<1.35*	≤
Avg.			.41	39	10 5	2.84	
3	concH_2SO_4	80	.42	32	7.7	2.08	6
7	concH_2SO_4	80	.41	39	10.5	2.84	6
14	concH_2SO_4	80	.43	39	11.1	3.00	6
Avg.			.42	37	9.8	2.64	
H_2SO_4 Avg.			.42	38	9.9	2.69	
4	Dropped in bath						
16	1:1 HCl	10	.44	59	16.0	4.32	6
17	1:1 HCl	10	.44	54	14.7	3.97	6
Avg.			.44	57	15.4	4.15	
4	1:1 HCl	15	.44	63	17.3	4.67	6
8	1:1 HCl	15	.43	58	16.5	4.46	6
9	1:1 HCl	15	.43*	44#	9.0*	2.43*	6
Avg.			.44	61	16.9	4.57	
6	1:1 HCl	20	.42	60	16.3	4.41	6
15	1:1 HCl	20	.44	56	13.8	3.73	6
18	1:1 HCl	20	.43	60	15.5	4.20	6
Avg.			.43	59	15.2	4.11	
HCl Avg.			.44	59	15.8	4.28	

Test Area 3 7 cm^2

*Not included in the averages

With any etchant the time was chosen so that approximately 0.5 mgms per cm^2 of CdS was removed from the film prior to the formation of the barrier layer.

Non-Aqueous Barrier Solution Studies

Moisture has a deleterious effect on CdS solar cells. Oxygen has been found to change the p-type character of Cu_2S. See appendix I. Complete removal of water and oxygen during processing would seem ideal. To accomplish this reduction or elimination it is necessary to substitute organic liquids or liquid salts for water. It must be kept in mind that the barrier formation reaction is essentially the substitution of 2 Cu^+ for Cd^{+2} in the film. The problem then is to make baths that provide cuprous ions.

Molten Salt Baths

Cuprous chloride molten salt systems were examined and several were found to have reasonably low eutectic melting points. Table IV lists some of the systems considered.

TABLE IV

Salt Systems

Salts	Approximate Eutectic Point	Approximate Composition
CuCl-NH_4Cl	120°C	40 mol % NH_4Cl
CuCl-KCl	130°C	65 mol % KCl
CuCl-RbCl	140°C	35 mol % RbCl
$CuCl_2$-$PbCl_2$	290°C	70 mol % $PbCl_2$
CuCl-NaCl	315°C	28 mol % NaCl
$CuCl_2$-$CaCl_2$	400°C	15 mol % $CaCl_2$
CuCl-LiCl	420°C	20 mol % LiCl

Those systems with eutectic melting points under 300°C were given serious consideration. Operation of such baths in the liquidus range was feasible. Continual use of such baths would gradually cause changes in the melting point.

Several of these systems were examined but were not adopted because the reaction rates were too high. Many times too large a portion of the CdS film was converted to copper sulfide. Reaction times were so short, of the order of a few

seconds, that reasonable control was difficult.

The only successful operation was the very rapid immersion and immediate retrieval of a 1 mil thick CdS film in the CuCl-KCl bath. No output was apparent until after lamination. The cell produced 0.43 volts and 14 ma for a 3 cm^2 substrate area. The problems were proportionally greater with increased bath temperatures.

The Conclusion is: Cells can be produced. The procedure is not presently practical because of:

a. Difficulty in controlling the reaction time.

b. Difficulty removing the film of frozen salts.

Recommendations:

(1) Development of a very low temperature bath with a eutectic point about 100°C by the study of 3 and 4 component baths. For example: a KCl-$AlCl_3$-CuCl bath should have a low melting point since KCl-$AlCl_3$ has a 115°C eutectic point. This will permit the use of reasonable immersion times.

(2) Development of such a bath as in (1) will make it possible to vary the copper concentration.

Organic Solvent Baths

The results of an exploratory test to determine the solubility of the salts, in some organic solvents are shown in Table V. Cuprous salts have low solubility in the high dielectric formamide, and in the low dielectric ethylene glycol. The addition of the corresponding sodium salt increases solubility. The formation of one or more complex anions is probably responsible. It was surprising that this effect was noted for ethylene glycol since such organics are seldom good solvents for inorganic salts.

CdS films were immersed in the baths listed in Table V to determine whether a Cu-Cd reaction takes place. The evidence was a dark layer on the CdS.

TABLE V

Solubility Tests in Organic Solvents

Solvent	Salt	Solubility & Remarks
Formamide	CUI	None at Room Temperature
Formamide	CuBr	None at Room Temperature
Formamide	CuI + NaI	Some at Room Temperature, Clear Blue
Formamide	CuBr + NaBr	Complete at Room Temperature
Formamide	CuCl + NaCl	Complete at Room Temperature Blue Solution
Ethylene Glycol	CuBr + NaBr	Some at Room Temperature After 2 Hours
Ethylene Glycol	CUI	None at Room Temperature
Ethylene Glycol	CuI + NaI	Soluble at Room Temperature

At room temperature, barrier regions were noted only for the complex baths. The formamide solutions were blue. The color may have been due to the formation of the cupro-ammonia complex since formamide contains the NH_2 radical. No photovoltaic output was noted for cells processed in this type of bath. The ethylene glycol formed yellowish solutions indicating the presence of the cuprous ion. Cells were fabricated from this type of bath.

After a 10 minute immersion in the formamide-bromide type bath a reaction was evident. Evidence of reaction occured after 15 minutes for the ethylene glycol type. No immediate photovoltaic effect was produced in either case. However, heating the cells made in ethylene glycol for 5 minutes at 200°C produced a slight power output.

With time a green layer formed at the surface of the formamide bath which gradually expanded toward the bottom indicating a rapid oxidation of the Cu^{+} to Cu^{+2}.

The ethylene glycol bath appeared to be worthy of continued investigation. At 120°C the bath was clear and colorless. This indicated a very low copper ion hydration level.

In order to determine what might be the best combination of salts and ethylene glycol, four combinationswere tried. These were NaBr+CuBr, NaI+CuI, LiBr+CuBr and LiI+CuI. There were about 150 cells made in these four baths. The times and temperatures of chemi-plating were varied. The results are summarized in Table VI.

Based on the results in these tests, the LiI+CuI in ethylene glycol appeared to be the most promising organic bath. This bath was used in all subsequent experiments. It consisted of 85 grams of LiI, and 70 grams of CuI in 100 ml of ethylene glycol.

Several experiments were made using this bath. Chemiplating times and bath temperatures were varied. The best conditions were found to be a 1 to 2 second immersion at 110°C to 120°C. Many cells were fabricated. In the majority of cases the open circuit voltage was close to 0.5 volts, and in some cases it

TABLE VI

Ethylene Glycol Barrier Baths

Bath	Best Cond.	Cells* Isc ma/cm^2	Comments
NaBr+CuBr	120°C, 2 sec., conc.	10 to 13	Some of best cells, but not very consistant results.
NaI+CuI	120°C, 1 sec., conc. or 70°C, 4 sec., conc.	5 to 9	
LiBr+CuBr	120°C, 2 sec., Dilute (10 gr CuBr, 12 gr Li Br in 100 ml E.G.)	5 to 10	
LiI+CuI	120°C, 2 sec., conc.	10 to 13	Most consistant results

* Cells were 1" x 1". Many cells were 5% or greater in spite of the rather low current densities.

was greater. The highest voltage attained was 0.55 volts. An example of the highest voltage cells is shown in Figure 9. Even though efficiencies as high as 5.4% were measured, the short circuit current remained low. The maximum current density was 16 ma per cm^2. Most cells made in the organic bath had current densities in the 10 to 14 ma per cm^2 range.

Elsewhere in this report the relationship between open circuit voltage and carrier concentration of the CdS film has been demonstrated. This relationship is shown for cells fabricated using the aqueous plating solution. Films of various carrier concentrations were plated in the organic bath and no definite correlation could be established. Films with carrier concentration in the range 5×10^{17} to 2×10^{18} per cm^3 yielded open circuit voltages of 0.5 volts or greater.

Because of the higher open circuit voltages the organic baths merit further investigation. An increase in current density will provide a superior cell.

Several tests were made in an effort to improve the current density. Various etchants were tried both before and after chemi-plating. These included HCl, H_2SO_4, and sulfur solvents. The standard method of pre-etching seemed to be of value when very long plating times were used.

The heat cycle after chemi-plating was varied. Low temperature heating up to 2 hours did not improve the cell although capacitance measurements indicated that wider junctions were produced.

One of the greatest advantages of the organic bath over the aqueous bath is the operating temperature. Temperatures well over 100°C minimize the oxidation of Cu^+ to Cu^{+2}. An experiment was conducted in which half of a group of films was protected from oxygen during processing. Completed cells revealed that the open circuit voltage was approximately the same in both groups. However, the current density was greater by a factor of 2 for the group protected from oxygen. This group yielded some of the highest current densities obtained

(16 ma per cm^2).

The areas for experiments are the concentration of the bath, the plating temperature, the plating time, the effect of oxygen, and the heating cycle after plating. The scope of the contract did not permit an exhaustive study.

Preformed Collector Grid Design

The current collector for the p-layer is composed of grid lines in the form of a screen. Several factors affect the collection efficiency. The final cell characteristics are affected by grid adherence, conductance, transmission, and quality of contact. A suitable grid was readily available but was too expensive. In an effort to find an equivalent but more economical grid certain problems were encountered.

Theoretical calculations [3] based on certain measured parameters of the electroplated barrier cell indicated that a grid with 20 lines per inch would be adequate. Experimental results at that time indicated that commercially available 70 lines per inch grids provided the highest cell efficiencies. These were electroformed precious metal grids. The best grid that a vendor could supply at a reasonable price was etched copper. A compromise at 50 lines per inch was chosen.

The vendor encountered problems in making a grid from the drawing submitted. (Figure 10). Fillets were necessary at each line intersection for strength. The specified transmission level could not be attained. It was also difficult to maintain the grid line width. Many of the grids received were below the required 85% transmission.

A thin layer of gold was plated over the grid before attachment to the barrier surface. This was necessary to isolate the barrier from the copper and to improve adherence. This caused a 5% loss in transmission.

Since the earlier calculations, many changes have been made in the process. These include modifications in film formation, barrier formation, and lamination.

Several 1" x 1" cells were made with various lines per inch

grids. (cf. Table VII). All cells were plated and processed identically and simultaneously. The data indicated that the heat cycle should be varied according to the grid spacing used. The 20 lines per inch cells were superior to those with the 50 lines per inch. The difference in efficiency was more than the 4% difference in transmission. It was noted that the 20 lines per inch gridded cells did not display a high series resistance.

Table VII Cell Data with Various Lines Per Inch

Cell	Grid	Trans	voc	Isc	Area	Eff.	
280-9	280 l/in.	67.5%	0.37v	27 ma	3.7 cm^2	1.3%	
313-8	280	67.5	0.34	28	3.7	1.0	
313-1	90	85.3	0.41	40	3.7	1.35	Poor Curve
313-2	50	85	0.42	50	3.7	2.84	
313-3	50	85	0.43	53	3.7	3.5	
313-4	50	85	0.44	48	3.7	3.2	
313-5	20	89	0.47	55	3.7	4.2	IV curve showed poor shunt resistance
313-6	20	89	0.47	57	3.7	4.0	
313-7	20	89	0.46	58	3.7	3.25	

The sheet resistance of several Hall samples of CdS was measured. Then a barrier was formed on the surface and the sheet resistance of the combination was measured. The Hall sample from film 313 (used in this test) measured only 630 ohms per square. The Hall samples from seven other films varied from 330 to 4400 ohms per square. When the sheet resistance of the CdS was compared to that of the CdS plus the barrier little difference was

noted. What this means is not clear. Another method of measuring the barrier sheet resistance is needed. A circuit similar to that used previously[4] where the potential is balanced along the underlying layer should clarify the results.

There was not sufficient time to complete these experiments. It does appear that, for certain films with lower sheet resistance values, cell power can be increased by reducing the number of grid lines per inch. (See Table VII)

Electrodeposited Grids

The electrodeposited grid technique is a method of applying a metal contact directly to the p-type cuprous sulfide layer. The grid used was a 70 lines per inch, square configuration which has an 85% optical transmission. Using a photoresist masking technique the grid was deposited on the p-type layer directly from a metal plating solution. Because of the intimate contact provided by this method, electroplated grid cells have been superior to all other types on thermal cycling tests. The main improvement resulted from the use of a non-cyanide gold plating bath. The cells from this bath were more uniform in electrical and physical characteristics.

Metals which act as diffusion barrier between the p-type cuprous sulfide and electroplated copper grid were investigated. Copper in direct contact with the barrier degrades the cell. Two interface metals, nickel and palladium, were found to be unsuitable because they had a deleterious effect on the cell output.

Up to this time efficiencies were low using either gridding technique (electroplating or thermo-compression). The thermo-compression type was favored because it did not entail an immersion of the cell in an aqueous solution and it did not require as much setup time. Thermo-compression grids were used exclusively during the remaining period.

Photoresist Masking

A variable speed, high torque spinner for photoresist application was designed and built. The turntable was equipped with a vacuum chuck. Using this spinner, thick uniform photoresist films with a few pinholes were produced. The best technique was found to be a multiple coat method using decreasing spinner speeds. Two coats of photoresist were applied, each followed by a 2500 rpm spin. Two additional coats were applied, each followed by 1000 rpm spin. The coated cells were then dried in an air convection oven at 60°C for 15 minutes. A Sylvania Sun Gun was used to expose the coating through a suitable mask for 90 seconds. A developer and water rinse completed the photoresist procedure.

Electroplating Solution

One of the difficulties encountered in electrodepositing grids is the degradation caused by immersing the cell in an aqueous solution. The power loss due to a short exposure to moisture is recoverable by heat treatment. Non-aqueous plating solutions were found unsuitable.(5) Therefore, aqueous baths must be used, but immersion times should be minimized.

At the beginning of the contract period the procedure consisted of an initial deposition of a thin 24K gold layer (0.2 microns thick) followed by a thicker layer (2.0 microns thick) of a high conductivity gold alloy. This procedure evolved because the pure gold bath required an extended time (45 minutes) to obtain a grid of proper conductivity. The gold alloy required only 12 minutes. However, the gold alloy does not make a good ohmic contact with the p-type layer. The initial pure gold layer provides protection while the gold alloy layer provides conductivity. The total immersion time for both processes was 15 minutes.

Both of the above baths were cyanide-complex types, buffered to prevent the formation of free cyanide. When a commercial non-cyanide gold bath became available, an investigation as to its suitability was begun. This is a high speed (15 minutes for 3 microns) pure gold deposit which has a remarkably good appearance even when plated on a surface as irregular as the barrier layer. As opposed to the two step method above, this non-cyanide process yielded shiny, well defined grids. The non-cyanide process was adopted as standard after a comparison test based on cell photo-

voltaic properties.

Two copper plating solutions, copper sulfate and copper fluoroborate were used to deposit grids. The Hull cell method was used initially to determine the optimum plating conditions (100 ma per cm^2) from the aspect of physical appearance. Cells plated at the normally recommended current densities invariably resulted in non-photovoltaic units with linear I-V curves. Heating after plating did not improve the units.

Both copper baths were then operated at the lowest current densities recommended and were finally diluted to permit further current density decreases (8 to 10 ma per cm^2 at 25°C). The best cells obtained had low open circuit voltages (0.2 volts) and poor grid adherence. These baths were investigated further in conjunction with the plating of palladium and nickel antidiffusion layers.

Antidiffusion Interface Metals

Although copper is more conductive and less costly than gold, attempts to utilize it as an electroplated grid metal have produced cells with low open circuit voltages. Spectral response measurements show that the copper reacts with the p-type cuprous sulfide layer converting it partially or wholly to cupric sulfide. An interface layer of a diffusion-preventing metal may avoid this problem. Two metals, palladium and nickel, were chosen.

Palladium was investigated first. Grids were electrodeposited in three ways: Standard 3.0μ Au; 0.2μ Pd plus 2.0μ Au; and 0.2μ Pd plus 2.0μ Cu. Compared to the standard gold, both groups of cells plated with palladium had 20-40% less short circuit current. Those plated with copper had 10-20% less open circuit voltage. Thus, palladium is not a desirable interface metal.

A similar series of tests were conducted using nickel. Because of low open circuit voltages nickel was also rejected.

Results

The best cell produced was a 44 cm^2 cell of 5.3% efficiency. The characteristics of the best cells are listed in Table VIII. It should be noted that the electroplating procedure was discontinued before a substantial number of high efficiency cells were produced by any gridding technique. For this reason, only a few 4% cells with electroplated grids can be listed, since only a few of the films processed were potentially 4% cells. Only 16 out of 116 electroplated grid cells had efficiencies above 3%.

TABLE VIII

ELECTROPLATED GRID CELL EFFICIENCIES

Cell No.	voc Volts	Isc ma	Pwr mw	Area cm2	Efficiency %
39c	.43	760	231	44	5.3
219D	.49	650	175	44	4.0
225D	.46	720	218	44	5.0
259C	.44	595	167	38.5	5.0
259D	.44	680	191	38.5	5.0
235-2	.43	700	202	47.5	4.3

Weight Reduction by Etching

Molybdenum of 2 mil thickness is used as a substrate to facilitate handling through lamination. After lamination, the excess molybdenum can be removed from the rear of the cell by etching. An acid spray etching chamber was used. Four 3" x 3" cells were etched simultaneously. The acid solution was sprayed against the exposed substrate surface for a period of about three minutes. Rinsing and air drying completed the process. The molybdenum thickness ranged from 0.3 to 0.5 mil after etching.

On the average, a finished 3" x 3" CdS cell [active area 44 cm^2] weighs 4 grams. After etching the average weight is reduced to 1.8 grams. The yields are exceedingly high. Efficiency and power output remain unchanged.

Pilot Line

Evaporation

Evaporation of CdS thin films has become a more controllable and better understood process as a result of changes in technique.

The method of preparation of the substrate was improved. Previously it was etched prior to the evaporation of the CdS. NASA noted, however, that cells which has been subjected to tests showed a separation of the CdS film from the substrate. This is detrimental to the performance of the cell, because of increased series resistance. Adherence was improved by sandblasting the substrates. This improvement should result in less damage during thermal cycling.

The nature of the CdS film, i.e., its physical and electrical properties, largely determines the performance of the solar cell. For this reason it was of great importance that control be achieved in evaporation, Prior to this contract, the evaporation parameters were standardized but the film was not sufficiently uniform. During this contract, steps were taken to improve their reproducibility. The carrier concentration and the resistivity of the film were taken as parameters. The most desireable range of carrier concentration for the best cells was from 5×10^{17} to 2 x 1018 per cm^3. Using undoped CdS powder, the carrier concentrations ranged from 1×10^{17} to 4×10^{18} per cm^3. With the standard evaporation technique no films were obtained with carrier concentrations in the range of 5×10^{17} to 9×10^{17} per cm^3. It was imperative that these values be achieved. By controlling the pressure in the bell jar during the evaporation these values of carrier concentration were attained.

A plot of the carrier concentration of the initial CdS film versus the open circuit voltage of the final cell shows a result of the present pilot line operation. See Figure 11.

Despite the effort made to control the physical characteristics of the films within a certain range of values, they still exhibit some individuality when made into cells. This is in part attributed to the fact that all Hall measurements are made on a film produced simultaneously on an insulating substrate. It is possible that the properties reported are not necessarily identical to those of actual film. Films treated simultaneously and in the same manner can give cells with different outputs. Occasionally, pieces out of the same 6" x 6" will vary. It was decided to take one 3" x 3" piece out of each film, cut it into nine 1" x 1"'s, and use these to determine the exact procedure of making the best cell from that film. The standard test consisted of determining the optimum plating times and the amount of heat the cell required prior to lamination.

The control of the carrier concentration of the CdS film and the "tailoring" of the heat prior to the lamination of the cell resulted in the increase of the efficiencies of 3" x 3"'s. Near the end of the reporting period, 50%of cells had efficiencies between 4.0 and 5.4%. The 1" x 1" cells had high efficiencies.

The majority ranged from 5.0 to 7.1%. See Table IX.

Gridding

The grid was changed from gold mesh to gold-plated copper mesh. The design of the grid (Figure 10) was altered so that spotwelding of the positive lead was eliminated. An extension of the grid itself became the positive lead. To ensure a good contact to the surface of the cell, the grids were attached by heat and pressure prior to lamination.

The gold-plated copper grids are thermo-compressed onto the cell by passage through heated rollers. (6) It was necessary to electroplate gold onto the copper mesh to improve the adherence of the grid and to prevent copper from contacting the barrier layer, since cells made with unplated copper grids were unstable. Two microns of pure gold were sufficient for adherence and stability. Bismuth, and gold alloy were tried as interface metals but were found unsuitable.

Lamination

Substantial progress was made in the laminating process. Previously, a combination of mylar-nylon was used, but this combination was not a satisfactory moisture barrier. Astrochemical cement. (7) was found to be a better moisture barrier and was substituted for the nylon. It was sprayed onto the mylar or Kaptan sheet. The composite plastic-epoxy was used as the encapsulant. This necessitated a change in the lamination cycle. Previously, the cycle was 15 minutes at 230°C. The exposure of cells to the high temperature of lamination resulted in excessive heat treatment. The temperature to cure the epoxy is 190°C. This was adopted as the new temperature of lamination with a 30 minute cycle time.

Cell Testing

A new simulated sunlight test setup was devised to measure cell performance in a manner consistent with that used by the contracting agency.

The test equipment incorporated a light source patterned after that used at Lewis Research Laboratory, NASA. (Figure 12) The lamps used were four 650 watt General Electric Sun Guns. The General Electric bromine type and the Sylvania iodine type sun guns were found to provide identical results. The General Electric

TABLE IX

CELL EFFICIENCIES

Film No.	Cell No.	Initial % Eff.	Time Interval Days	Final % Eff.
93	93-27	4.3	3	3.6
	-28	4.2	3	4.4
	-29	4.7	3	4.8
	-30	5.3	3	5.5
	-31	5.6	3	5.6
	-32	5.6	3	5.7
	-34	7.1	3	7.1
113	113-12	6.3	1	6.2
	-13	6.0	1	6.0
	-14	4.7	1	4.5
	-15	6.0	1	6.0
	-23	5.2	1	5.2
	-17	5.6	7	5.3
	-18	5.5	7	5.0
	-19	5.4	7	4.5
	-20	6.3	7	5.3
	-21	4.9	7	4.0
	-22	6.4	7	6.0
117	117-6	5.2	1	5.1
	-7	5.5	1	5.4
	-8	4.7	1	4.6
	-9	5.3	1	4.2
	-12	6.7	1	6.7
	-11	6.2	1	6.2
	-14	7.0	1	7.0
101	101-1	5.3	6	5.3
	-2	5.3	6	5.3
	-4	5.2	6	5.2
	-5	5.4	6	5.4
	-7	5.3	6	5.3
	-8	5.2	6	5.2
	-10	5.1	6	5.1
	-11	5.6	6	5.6

Note: Efficiencies based on a grid area of 3.7 cm^2. For a 7.0% cell the efficiencies would be 5.8% for a 4.5 cm^2 substrate area; and 8.3% for an active area of 3.1 cm^2. All cells had thermo compressed gold grids except those marked* which had thermo compressed copper grids.

lamps were selected because of their convenient size, shorter filaments, and higher power. The shorter filaments are closer to being a point source.

The second important part of the test set-up was the filter. It consists of a lucite box with two 12" X 12" windows which are 2" apart. The space between the windows is completely filled with 0.1% copper sulfate solution. It has a reservoir in the rear to supply solution to compensate for evaporation. In addition a pyrex plate was mounted over the filter box to reduce the infrared. The cells used for standardization were calibrated by NASA. The I-V data was taken from an oscilloscope or an x-y plotter.

Results

Of the 800 3" x 3" cells made on the pilot line, 450 were delivered to Le.R.C. These figures do not include cells made for other contract purposes. Each major fabrication step was studied and modified for optimum cell output. The final result was the production of cells ranging from 4.0% to 5.4% with a yield rate of about 50%. An I-V curve of a typical 5% cell is show in Figure 13. This result was confirmed at LeR.C. The highest efficiency cell [3.4 cm^2] obtained in the laboratory was 7.1%. The I-V curve is shown in Figure 14. A plot of the cell efficiencies for the contract period is shown in Figure 15.

An engineering drawing of the particular cell construction used during the investigation is shown in Figure 16.

REFERENCES

1. Nicoll, F. H. The Use of Close Spacing for Growing Epitaxial Layers of Semiconductors, Journal of Electrochemical Society, November 1963 Vol. 110, No. 11 page 465.

2. Hass, G. and Thun, R. E. Physics of Thin Films Vol. 3, page 170

3. Technical Documentary Report No. ASD-TDR-62-69 Research on Solar Energy Conversion Employing Cadmium Sulfide Vol. II December 1962, page 16

4. Griffin, T. A., Olmsted, R. W., Schaefer, J. C., Research and Development in CdS Photovoltaic Film Cells NASA CR-54108, June 1964, page 33

5. Griffin, T. A., Krus, D. J., Schaefer, J. C., Research and Development in CdS Photovoltaic Film Cells NASA CR-54481, August 1965, page 19

6. Harshaw Proprietory Process

7. Thermosetting Epoxy Adhesive BP242-4A-2, Astrochemical Company, Schenectady, New York

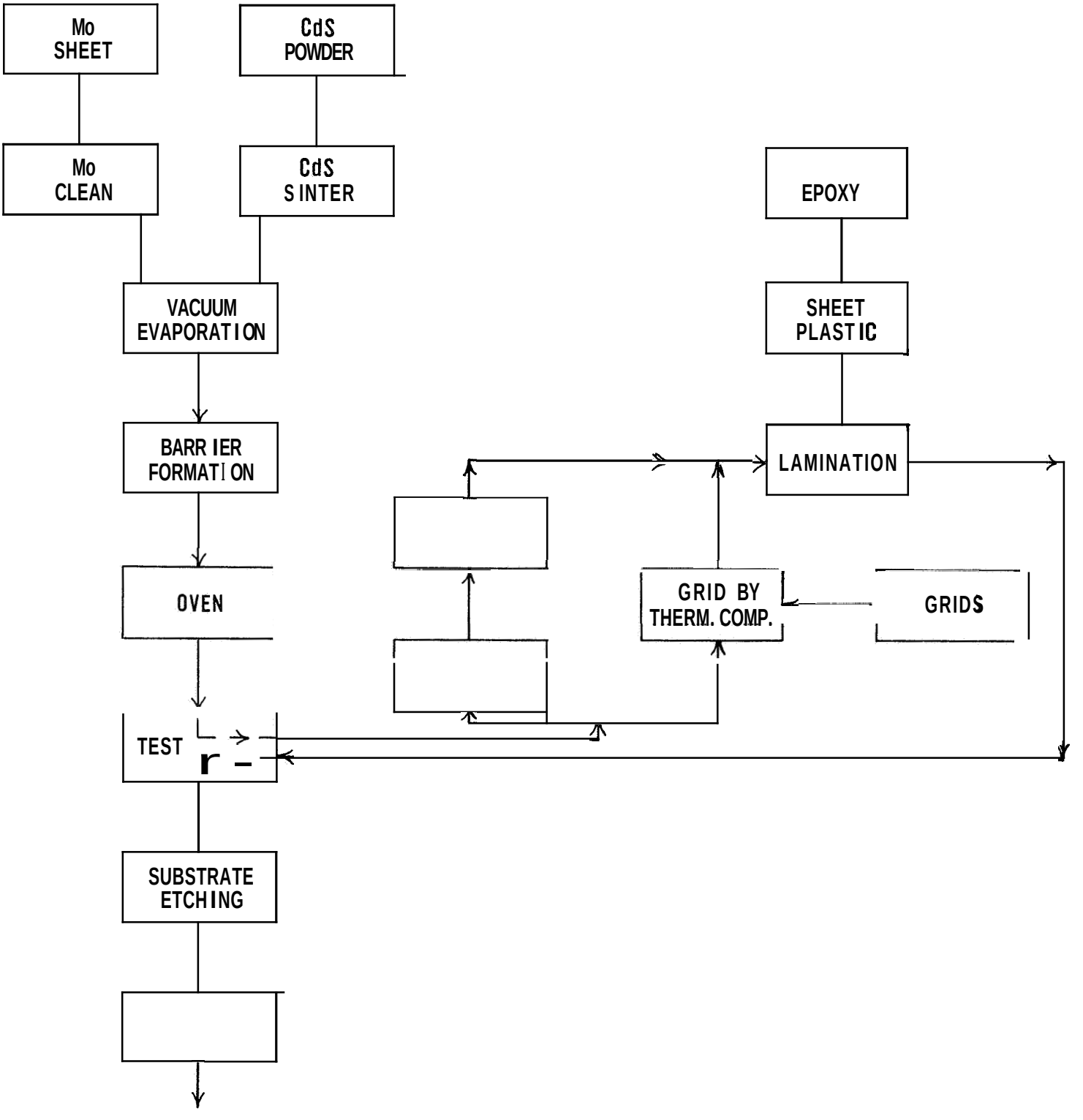

Figure 1 FLOW DIAGRAM OF CELL FABRICATION

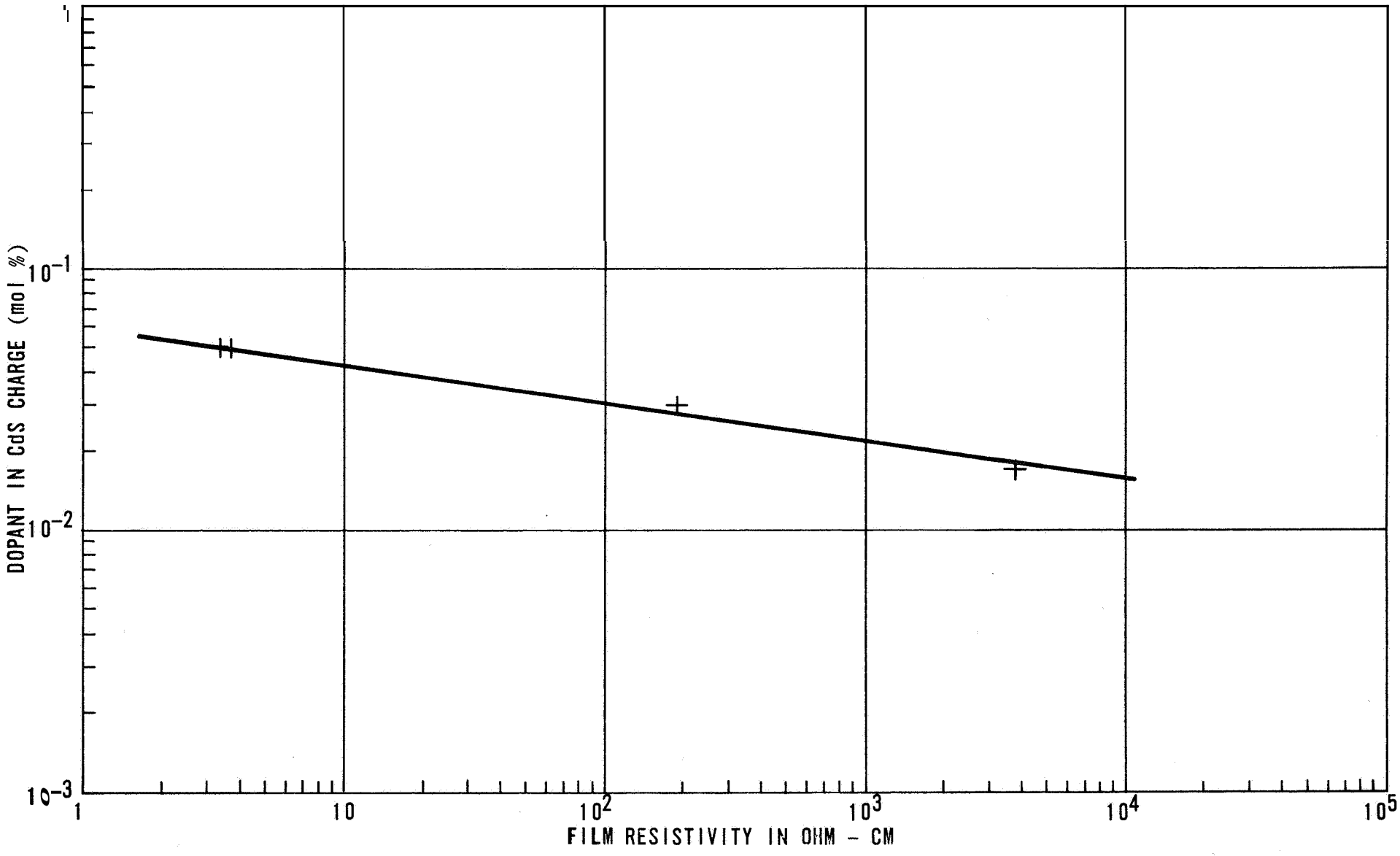

Figure 2

FILM RESISTIVITY VS DOPANT FOR VAPOR TRANSPORT FILMS

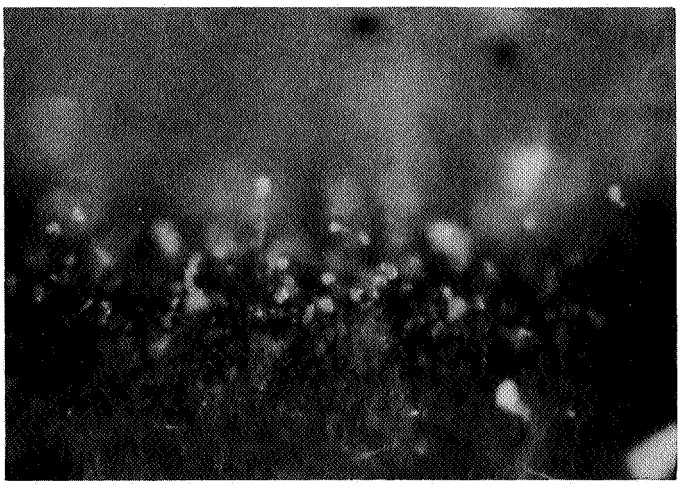

140X Photomicrograph of Whisker Growth on Vapor Transport Film

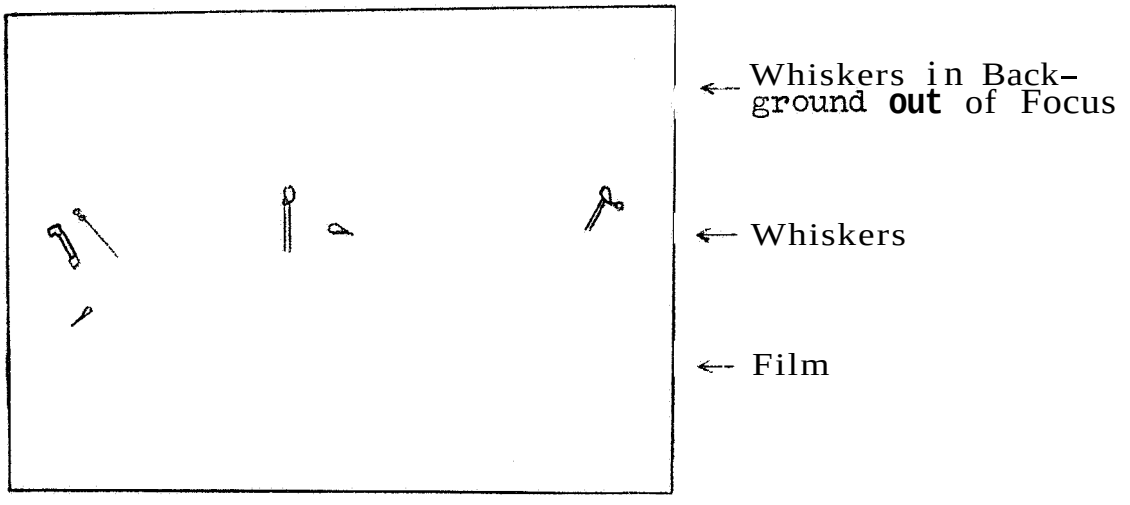

Figure 3 WHISKER GROWTH ON VAPOR TRANSPORT FILM

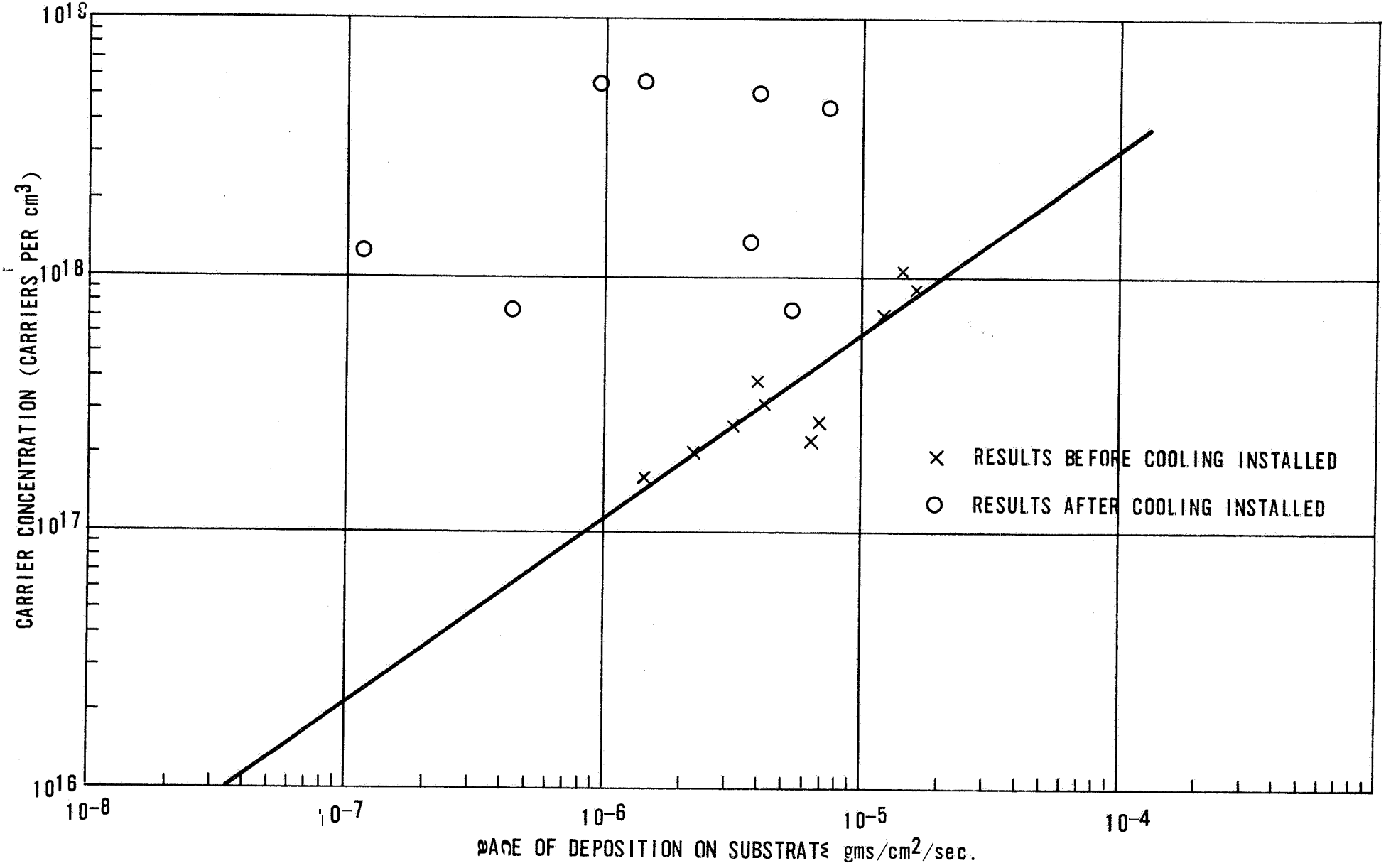

Figure 4 CARRIER CONCENTRATION VS RATE OF DEPOSITION

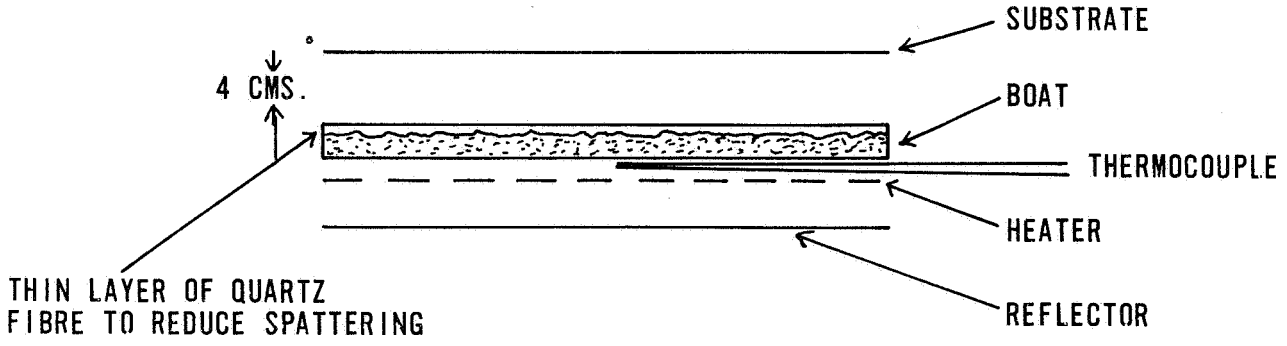

Figure **5**

CLOSE SPACE5 SAMPLE AND SOURCE CONFIGURATION – DOPANT STUDY

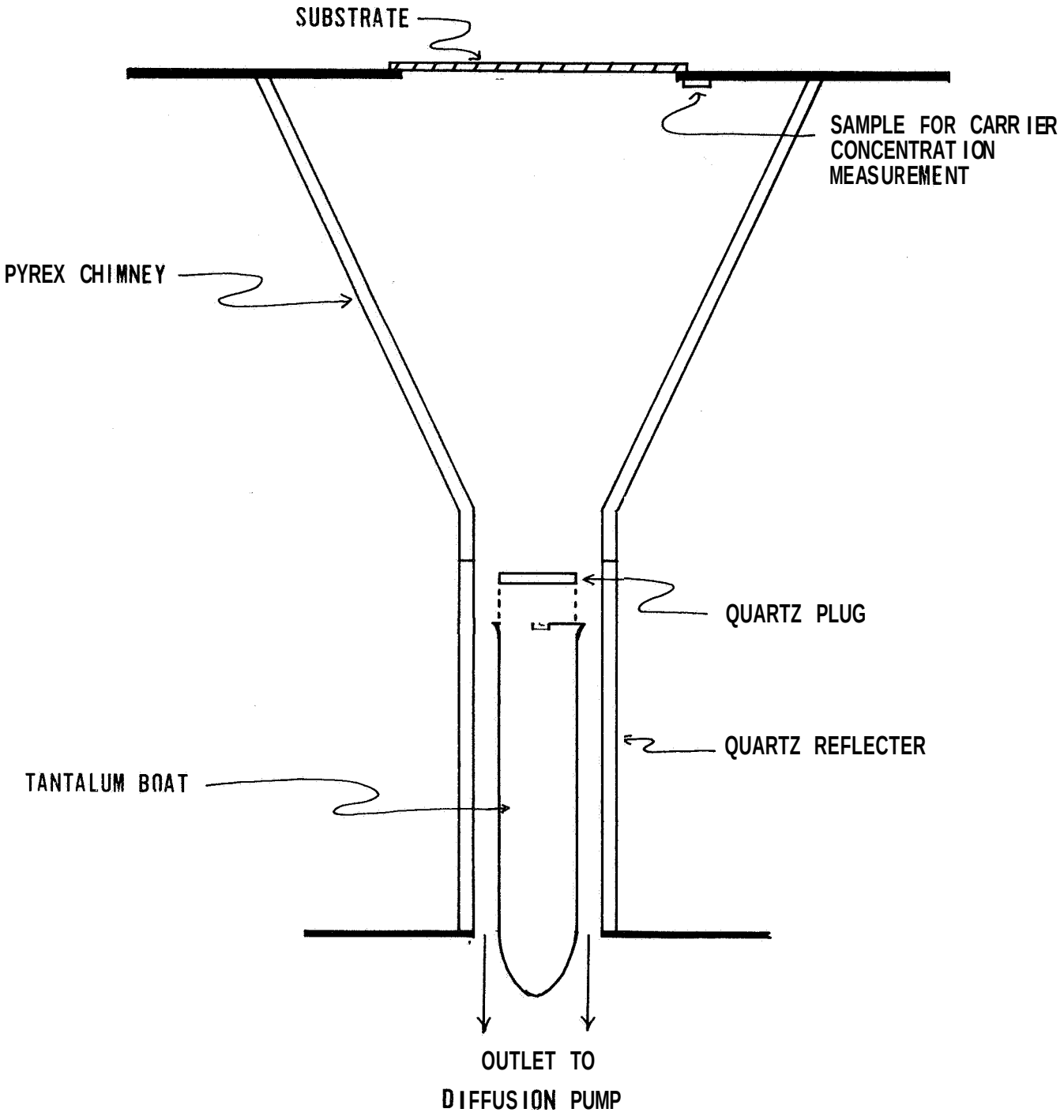

FIGURE 6

EVAPORATION SAMPLE AND SOURCE CONFIGURATION - DOPANT STUDY

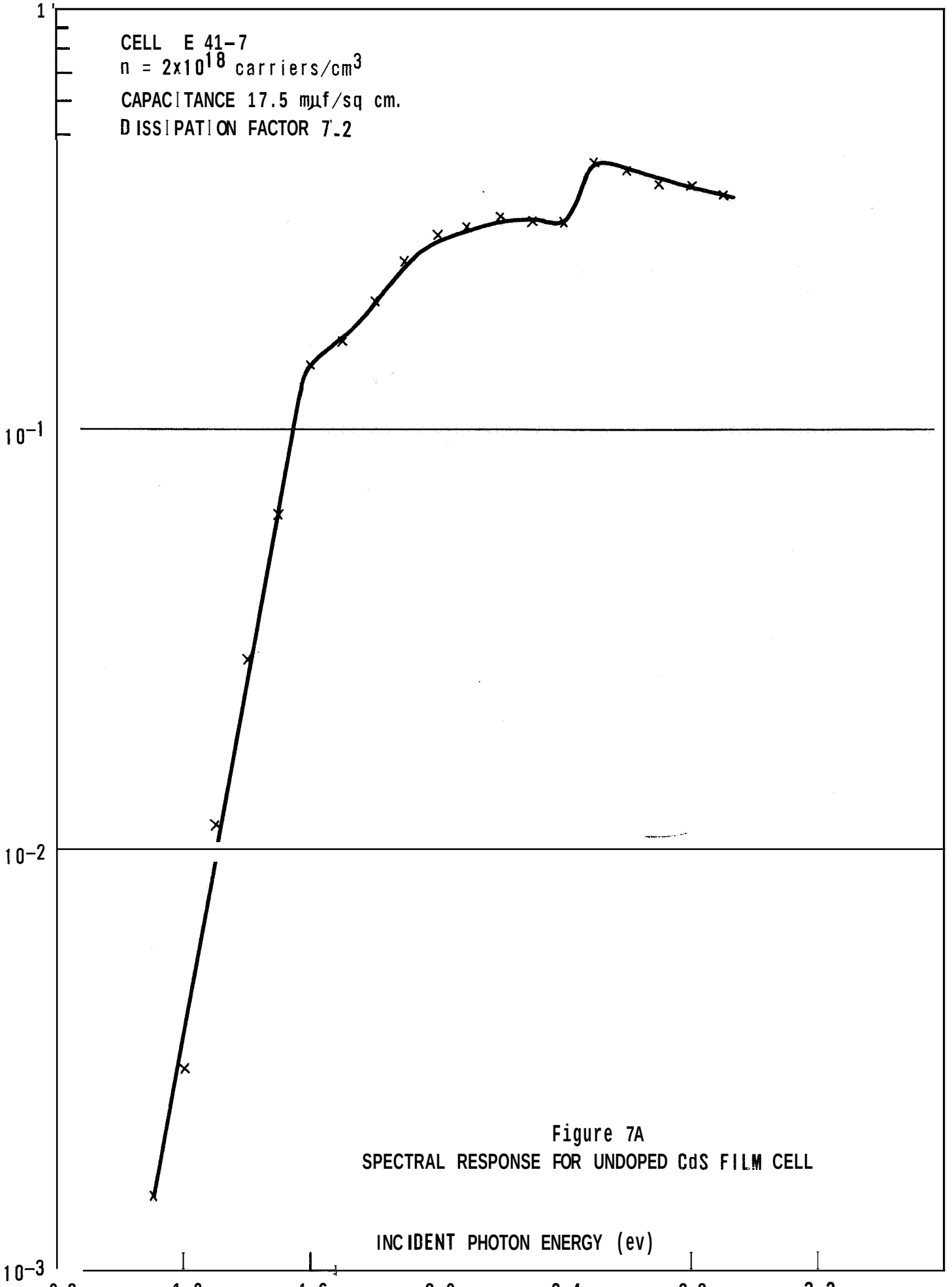

Figure 7A
SPECTRAL RESPONSE FOR UNDOPED CdS FILM CELL

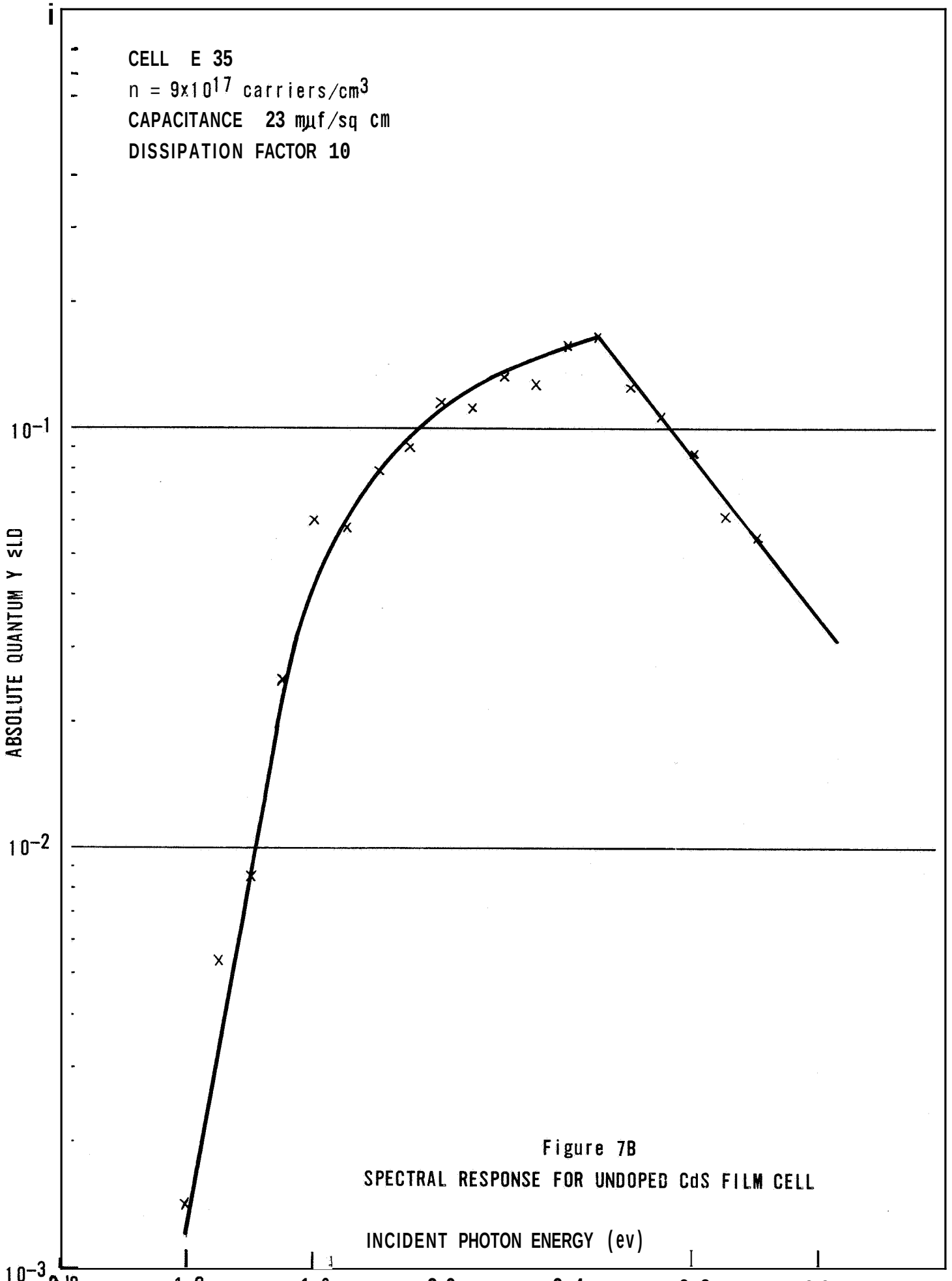

Figure 7B

SPECTRAL RESPONSE FOR UNDOPED CdS FILM CELL

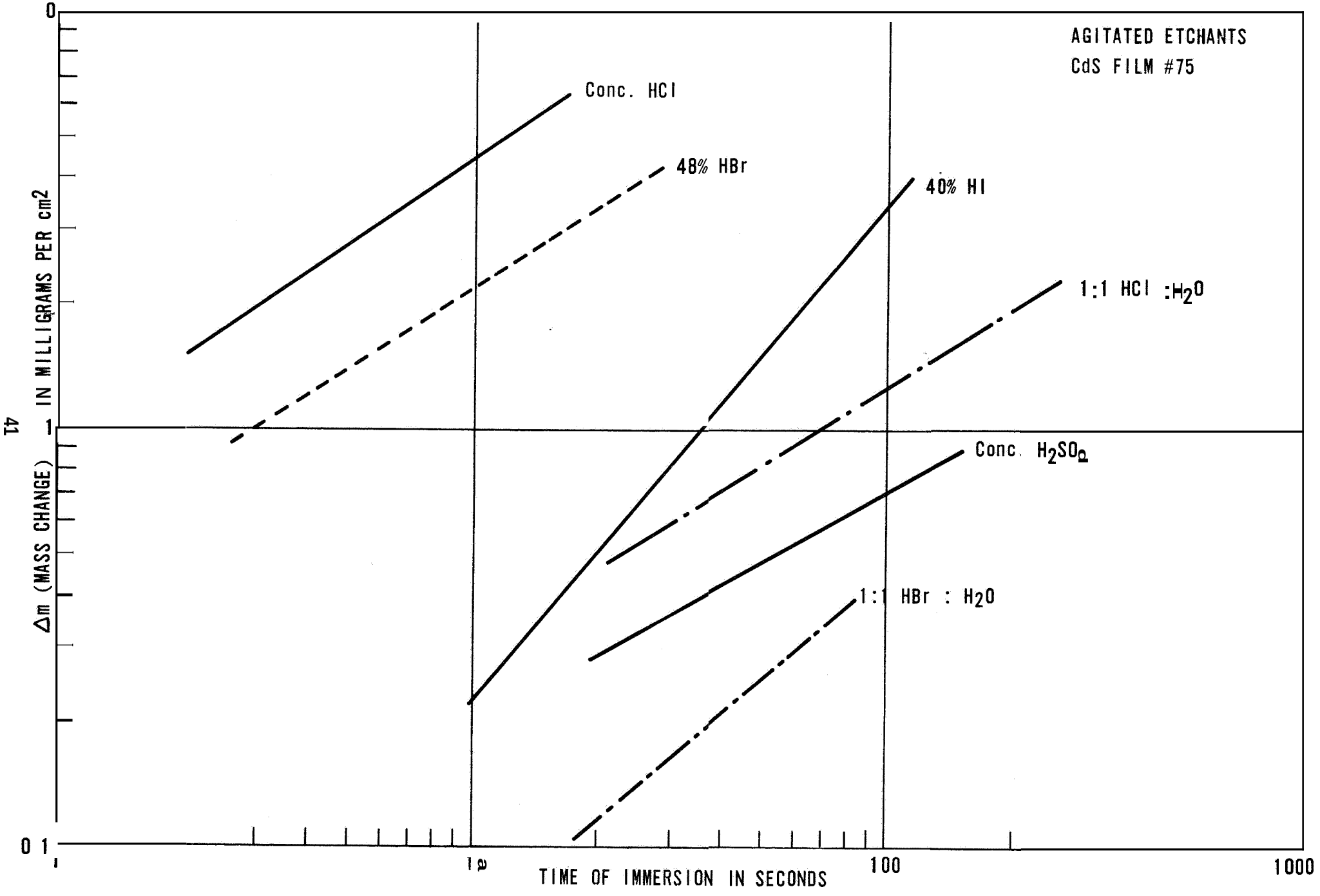

Figure 8 MASS CHANGE VS ETCHING TIME

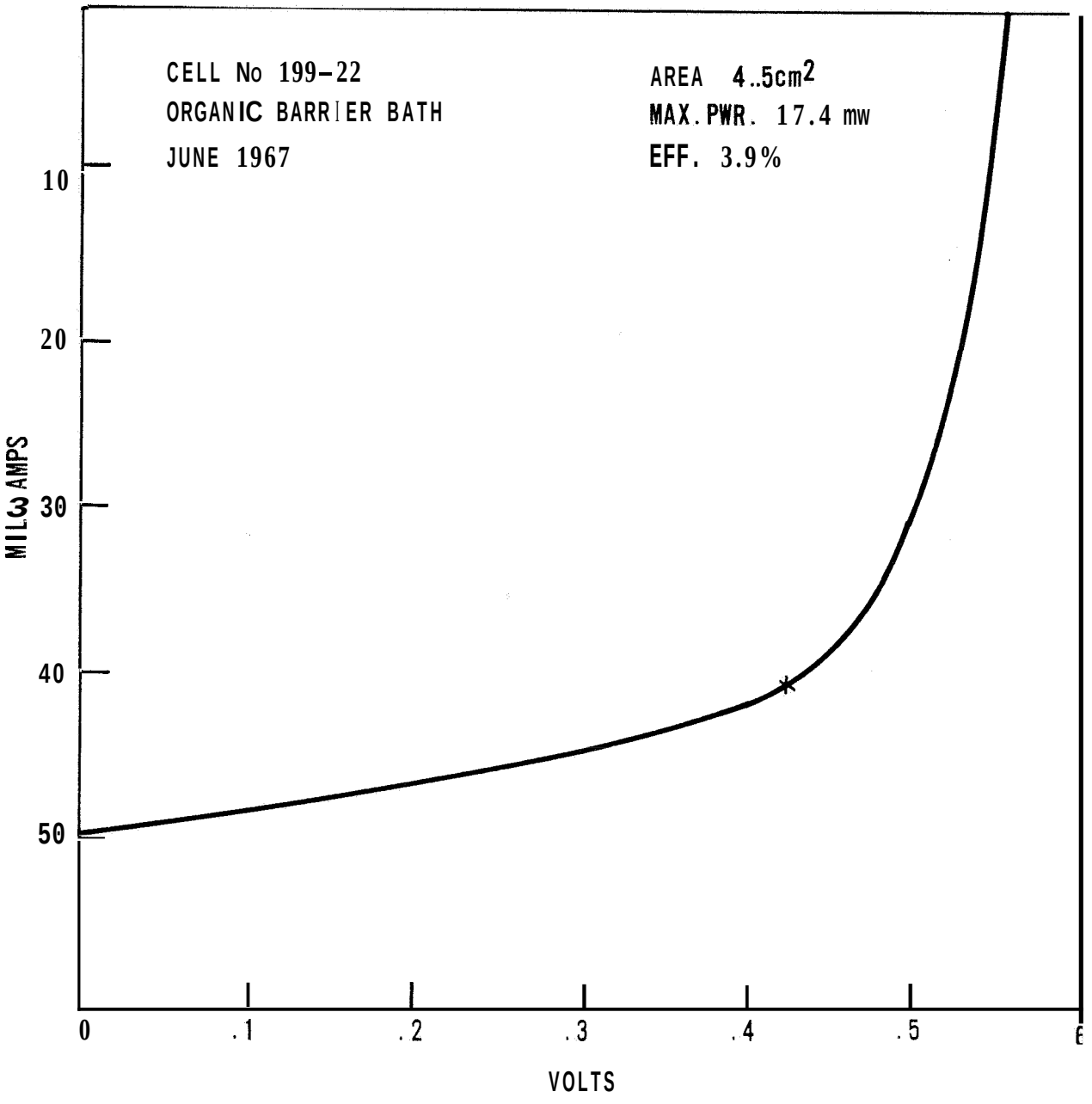

Figure 9 I-V CURVE OF CELL FROM ORGANIC BATH

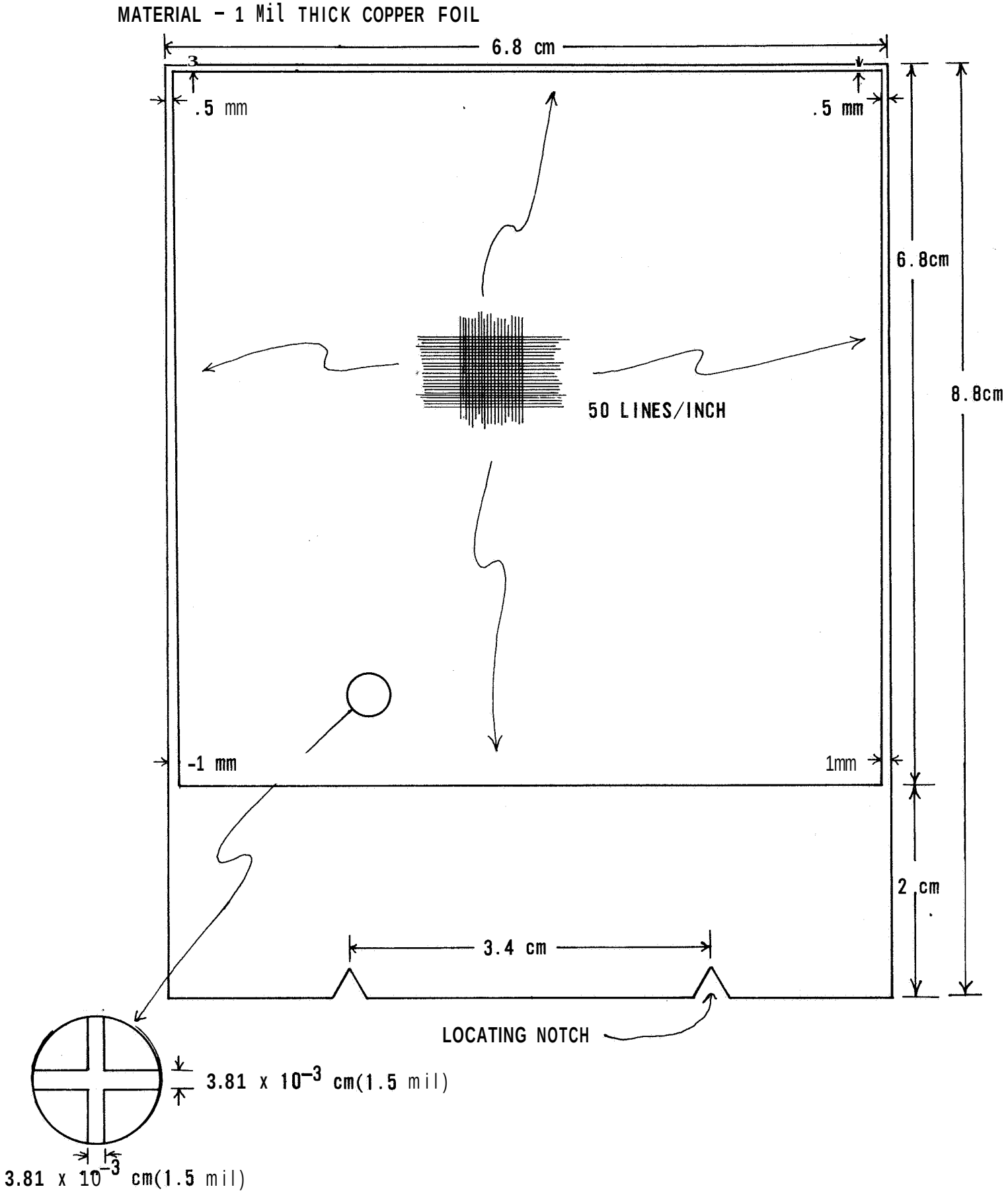

Figure 10 CELL GRID DESIGN

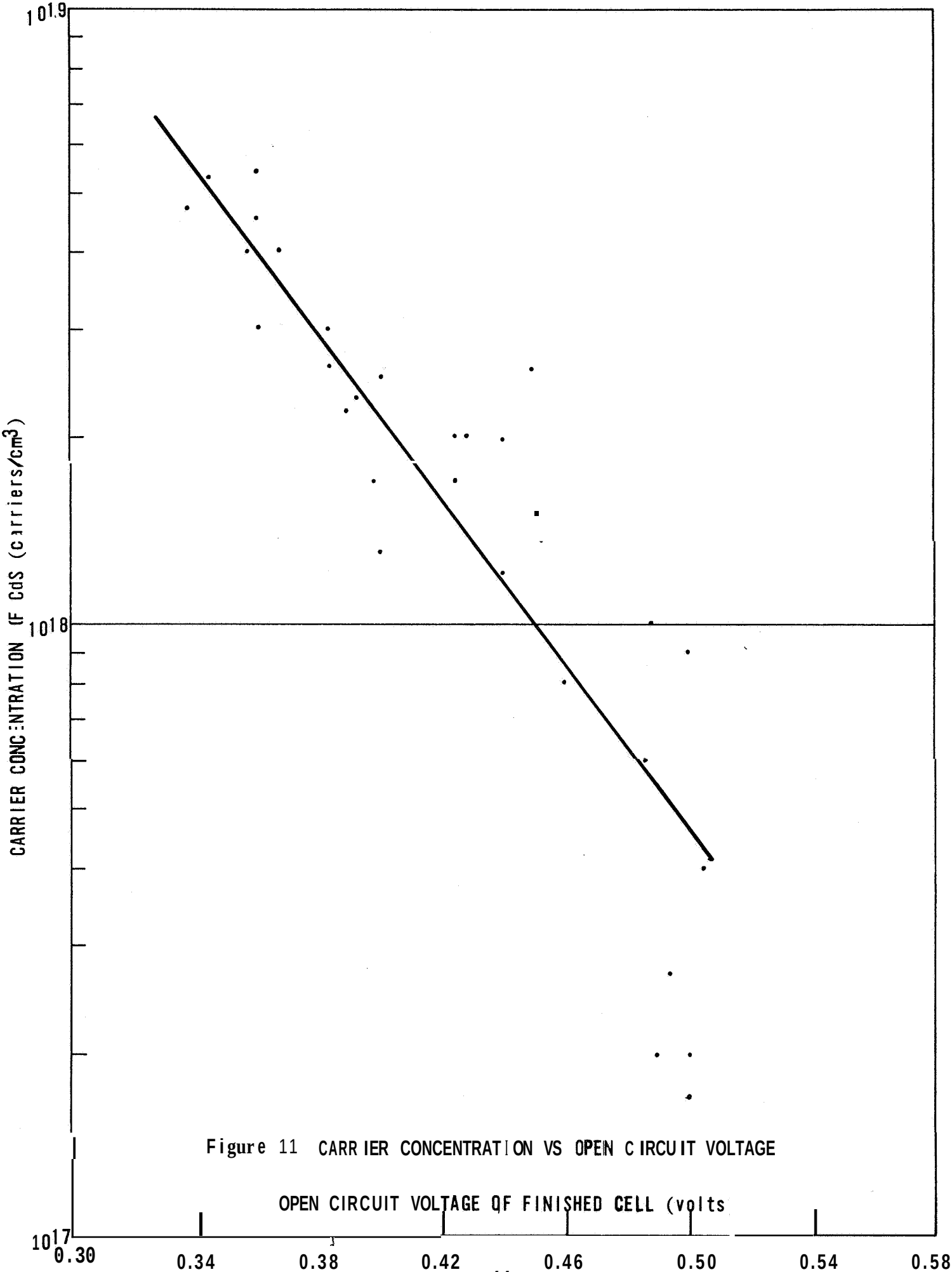

Figure 11 CARRIER CONCENTRATION VS OPEN CIRCUIT VOLTAGE

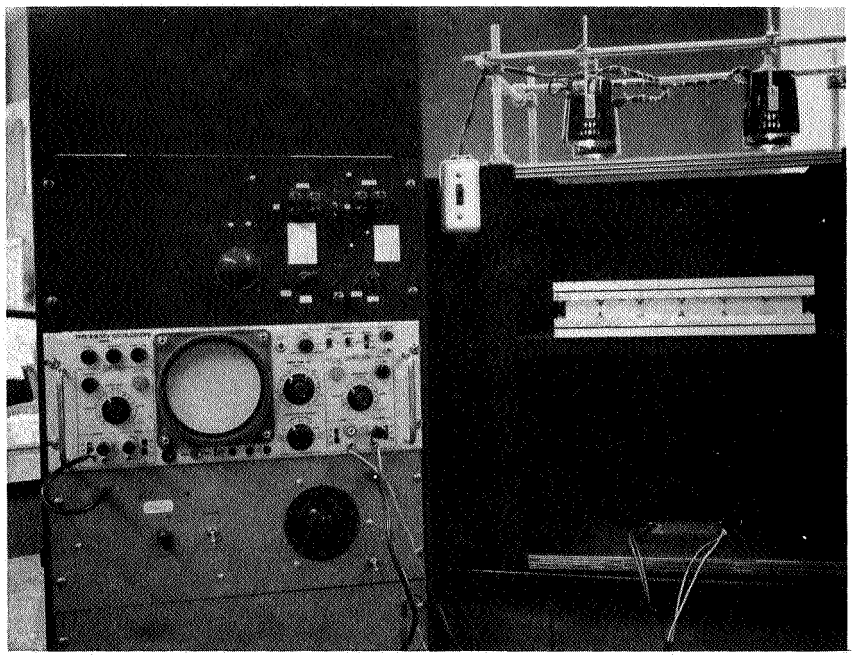

Figure **12** SIMULATED SUNLIGHT TEST APPARATUS

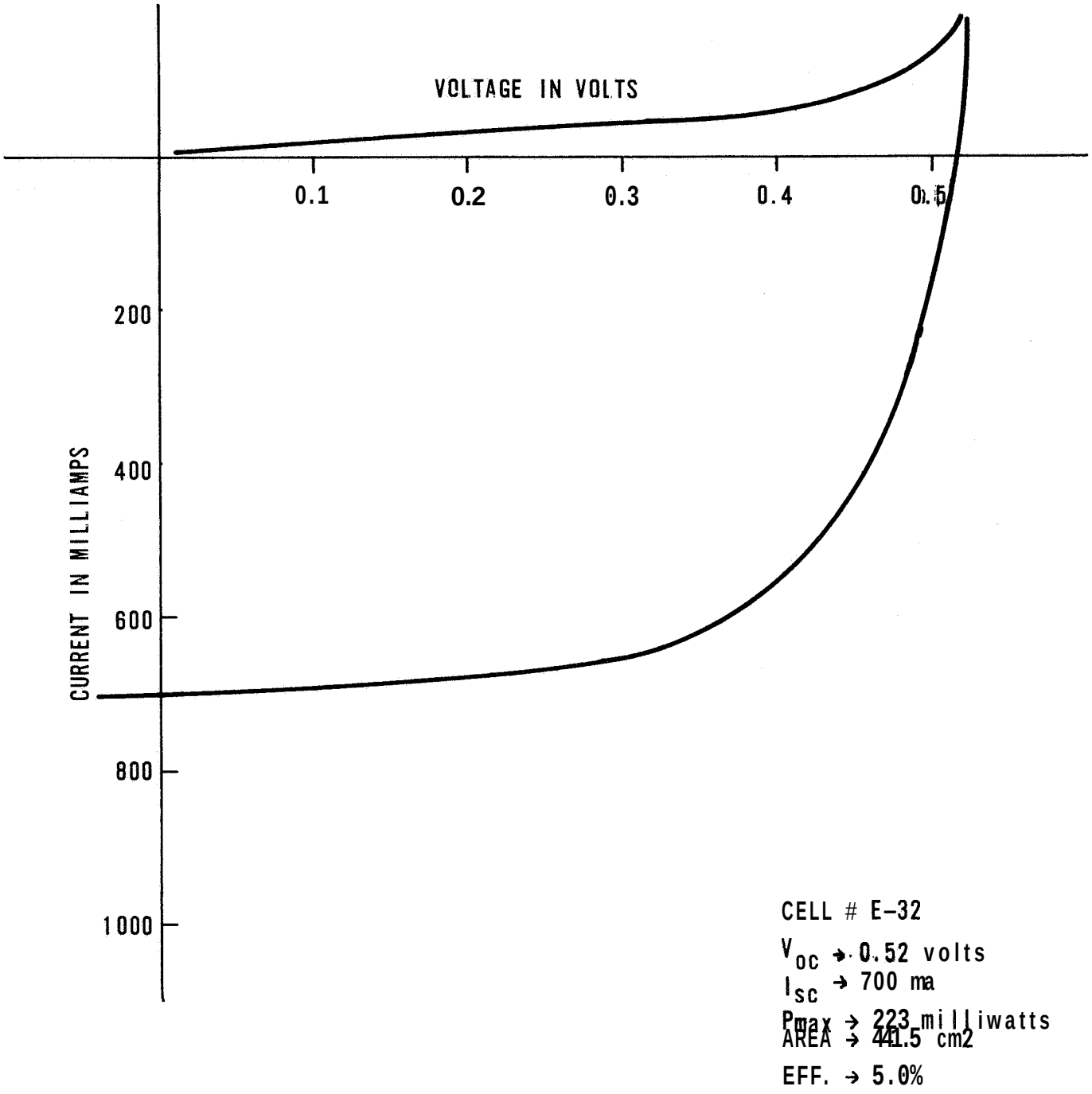

Figure 13 I-V CURVE OF TYPICAL 5% CELL

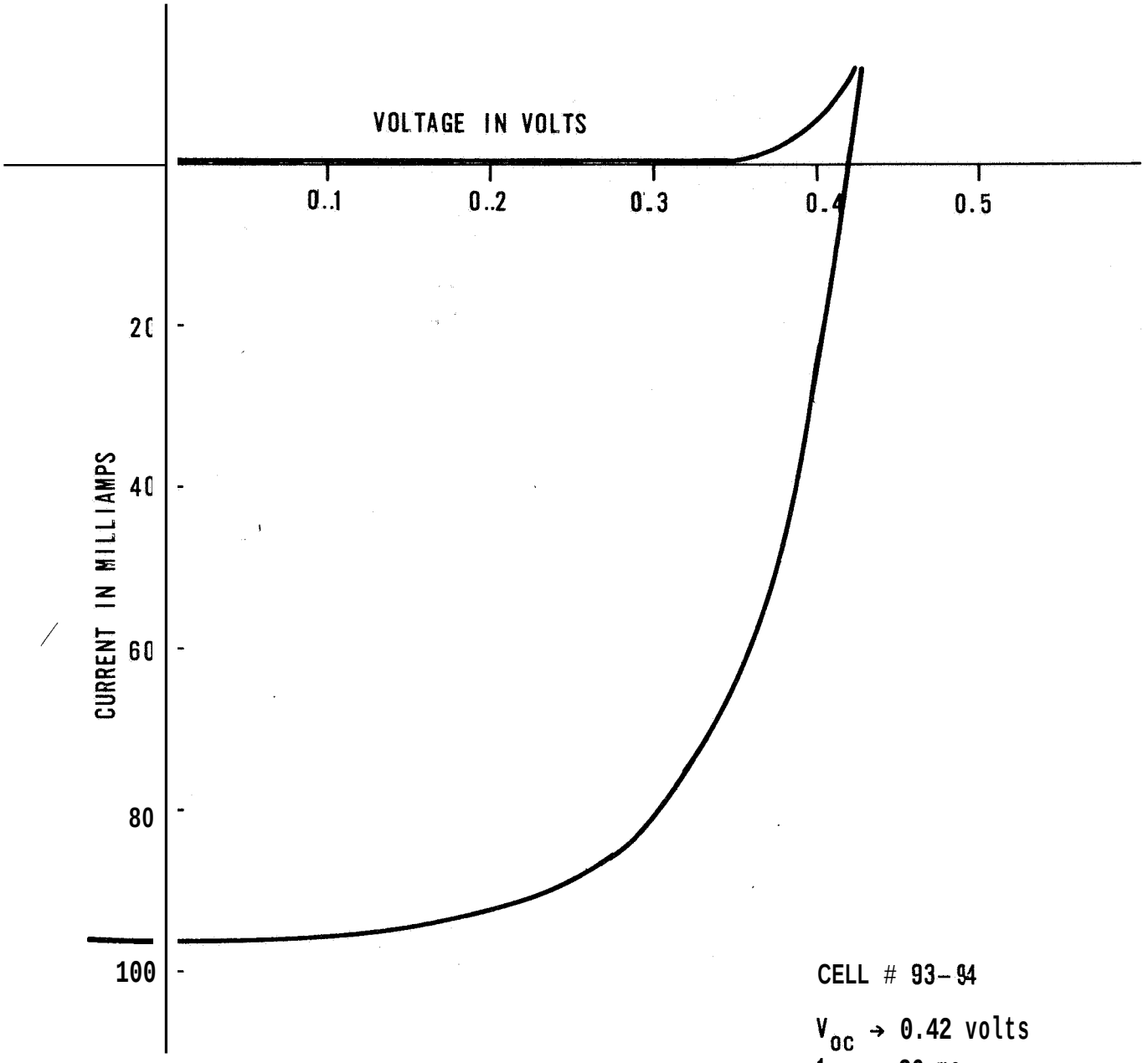

Figure 14 I-V CURVE OF 7.1% CELL

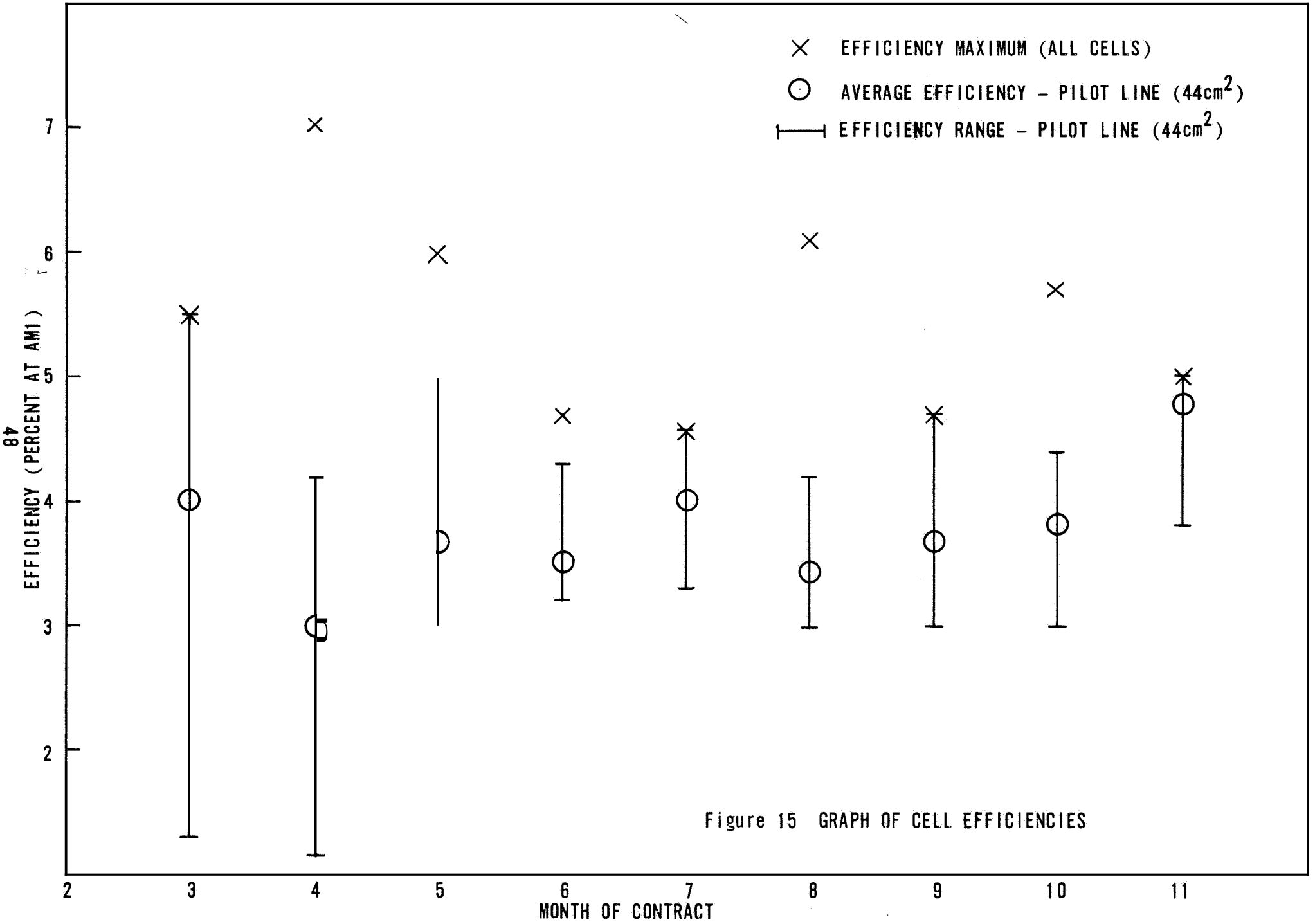

Figure 15 GRAPH OF CELL EFFICIENCIES

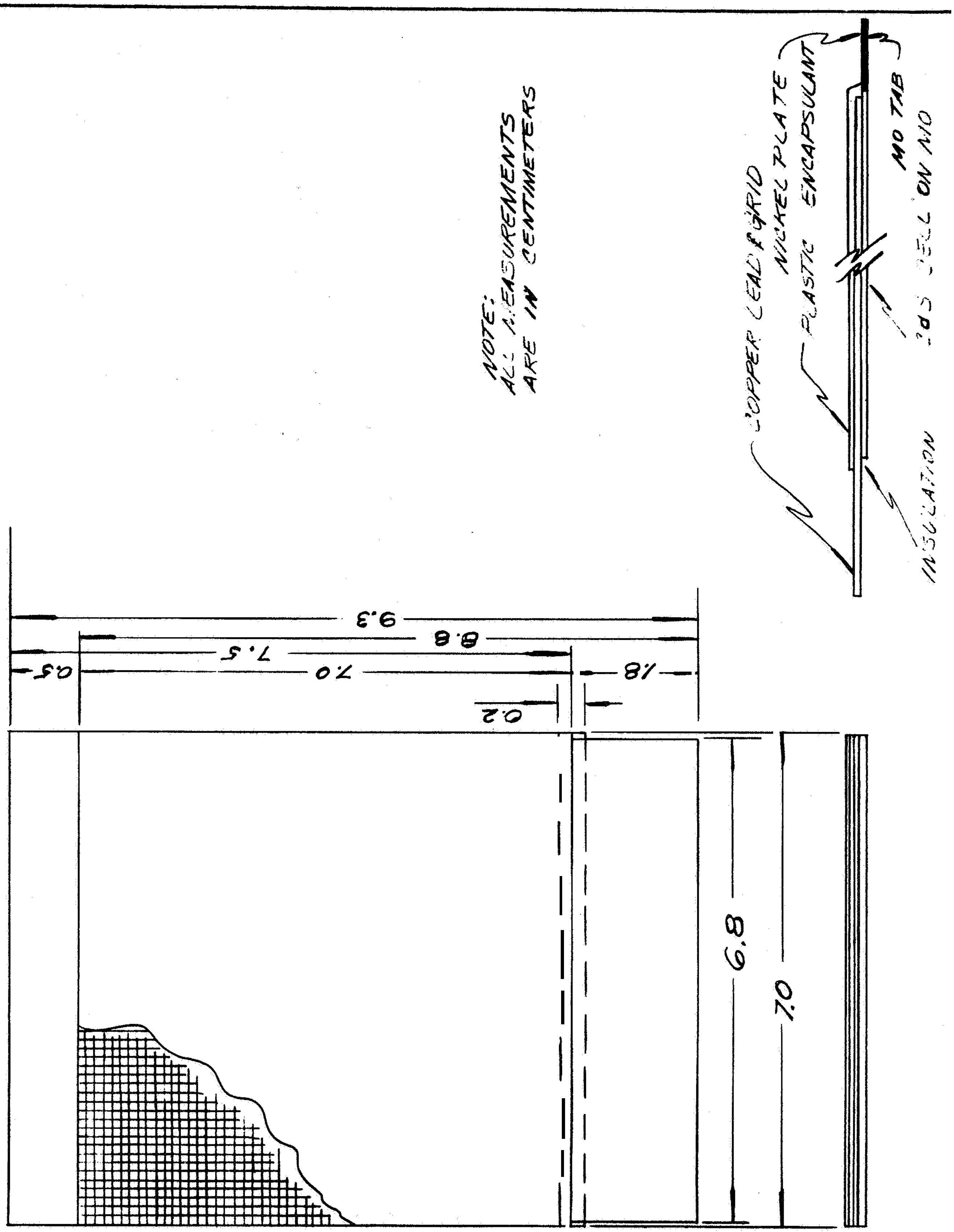

REV.	CHANGE	DATE

DR. D. H. | CH. | APP.

THE HARSHAW CHEMICAL CO.

1945 EAST 97TH ST. CLEVELAND, OHIO

CRYSTAL DIVISION

TITLE Figure 16

'DRAWING , F CdS SOLAR CELL ON MOLYBDENUM

MATERIAL

TYPE NO.

DWG NO.

HARSHAW 645

APPENDIX I

FURTHER CONSIDERATIONS ON THE MODEL FOR THE CdS SOLAR CELL

BY

E.R. Hill, B.G. Keramidas, and D.J. Krus

FURTHER CONSIDERATIONS ON THE MODEL FOR THE CdS SOLAR CELL [1] [2]

E.R. Hill, B.G. Keramidas, D.J. Krus
HARSHAW CHEMICAL COMPANY
Division of Kewanee Oil Company

Introduction

This paper proposes a model for the CdS solar cell which accounts for all the major features. It uses only physically evident material properties and does not require traps or metastable states. Our conclusion is that, in fact, traps are physically mobile impurity ions.

The cell itself is a p-n junction whose characteristics are altered by the presence of mobile impurity ions. It is proposed that the structure consists of n-type CdS in and on which p-type Cu_2S is grown, and that the rectifying junction changes geometry and characteristics due to ion motion in applied electric fields. This is in contrast to normal semiconductor diodes where p and n materials are in contact, but the impurity ions are assumed to be fixed. The model supposes that both CdS and Cu_2S are semiconductors to which simple band theory can be applied. The mobile ions provide the only deviation from standard p-n junction theory and give rise to all anomalous behavior. After a brief description of the device, the discussion divides into four sections:

1). Properties of CdS
2). Properties of Cu_2S
3). Evidence for and mobilities of ions
4). Microscopic picture of junction formation and behavior

Description

The CdS solar cell is a heterojunction between semiconducting CdS and Cu_2S. The CdS is n-type single crystal or polycrystalline evaporated film. The Cu_2S is p-type and is

(1) This work was supported by a grant from the Harshaw Chemical Company and in part by NASA, Lewis Research Center.
(2) Paper presented at IEEE Sixth Photovoltaic Specialists Conference, March, 1967.

chemically formed from a portion of the CdS. The impurity ions in these two materials have high mobilities by solid state standards, producing many unusual properties. A schematic physical picture is shown in Figure 1.

I. Properties of CdS

The CdS used in this device is a conductive single crystal or an evaporated thin film. It has the characteristic optical absorption edge at 2.4 ev which means that a periodic structure must be present. Hall and Seebeck coefficient measurements show n-type conductivity with carrier concentration ranging from $10^{15}/cm^3$ to $10^{20}/cm^3$. Mobilities in the crystal are about $200 cm^2$/volt-sec. and about 1 to 10 cm^2/volt sec. in the evaporated film. Consequently, resistivities will range from 10^{-2} to 10^2 ohm-cm. P-type CdS has never been reliably observed despite considerable effort and diligent searching. Consequently, this will not be considered as part of the cell.

II. Properties of Cu_2S

Cu_2S is always made from a portion of the CdS by chemical reaction. The reaction is described by:

$$CdS + 2Cu^+ = Cu_2S + Cd^{++}$$

It can be carried out in a number of ways, such as by immersing CdS into an aqueous solution of cuprous chloride. Evidence that Cu_2S is indeed the product is found by simple weighing processes. CdS powder is weighed and then treated with the cuprous ion solution. It is dried and weighed again. The resulting powder is etched with KCN-water which does not affect CdS, but removes copper and its compounds. This residue is dried and weighed. Two copper atoms weigh 15 grams/mole more than one cadmium atom, so the powder gains weight in the reaction. The weight loss in the KCN etch is the weight of the Cu_2S formed, which is 159 grams/mole. The data for the experiment is:

CdS mass	= 12.0512 gm	
Powder mass after reaction	= 12.4250	
Mass change	= + .3738	= 2Cu-Cd
Mass change in KCN rinse	= -3.4170	= $-Cu_2S$

$$\frac{\text{Mass change in KCN}}{\text{Mass change in reaction}} = \frac{-3.4170}{+.3738} = -9.2$$

This same ratio when calculated for the displacement of a Cd^{++} by $2Cu^{+}$ is $\frac{-Cu_2S}{2Cu-Cd} = \frac{-159}{15} = -10.6$

Clearly, this material is Cu_2S.

If a solution containing cupric ions is used, such as $Cu(NO_3)_2$ and water, the resulting product is cupric sulfide. This is proved by repeating the previous experiment. In this case the powder loses weight, since one copper atom weighs less than one cadmium atom. The data is as follows:

$$Cu^{++} + CdS = CuS + Cd^{++}$$

CdS mass	= 12.5240 gm
Powder mass after reaction	= 11.2910
Mass change	= -1.2330 = Cu-Cd
Mass change in KCN rinse	= -2.6610 = -CuS

$$\frac{\text{Mass change in KCN}}{\text{Mass change in reaction}} = \frac{-2.6610}{-1.2330} = +2.16$$

The calculated ratio fox the displacement of a Cd^{++} by a Cu^{++} is $\frac{-CuS}{Cu-Cd} = \frac{-95.5}{-48.9} = 1.96$

Clearly, this material. is CuS.

The solar cell using Cu_2S shows a strong spectral response in the infrared with an absorption edge at about 1 ev, as shown in Figure 2. The shape of this edge is typical of a semiconductor and is sufficient to show the presence of a lattice structure. Further evidence for semiconduction is found in Seebeck coefficient and resistance measurements. Figure 3 shows the steps in this process. A CdS film is evaporated onto an insulating substrate. Its Seebeck coefficient and resistance are measured. Next a layer of Cu_2S is formed and the Seebeck coefficient and resistance of the combination are measured, being sure that the CdS and Cu_2S are both connected to the end electrodes. The Cu_2S is then etched off with RCN and the Seebeck coefficient and resistance of the remaining CdS are measured. The Seebeck coefficient of the initial and remaining CdS was the same in all experiments.

The analysis of this data is carried out by considering the CdS - Cu_2S combination as two thermoelectric generators with internal resistances connected in parallel. The equation for this

is also shown in Figure 3. This has shown the Cu_2S always to be p-type and with a carrier concentration of 10^{18} to $10^{19}/cm^3$. Resistivity can be calculated knowing the thickness of the initial film, and the result is usually about 10^{-1} to 10^{-2} ohm-cm. n-type Cu_2S has never been observed.

The carrier concentration of the Cu_2S depends on the original CdS which is n-type because it contains donor impurities, These donors do not enter into the chemical reaction and are incorporated in the Cu_2S layer. They will also act as donors in Cu_2S, reducing the hole concentration and conductivity. High donor concentration CdS produces low conductivity Cu_2S and the parallel combination shown in Figure 3 has bower conductance than the initial CdS. Lower donor concentration CdS, produces high conductivity Cu_2S. The parallel combination has a higher conductance than the initial CdS. Data from these experiments indicates the chemically formed Cu_2S to have a carrier concentration in the range of 10^{18} to $10^{19}/cm^3$. If the CdS - Cu_2S combination is heated in vacuum, nitrogen, or argon, the room temperature resistance is increased, indicating a diffusion of the Cu_2S acceptors into the bulk. However, if heating is carried out in air or oxygen, the resistance decreases. The resistance of the Cu_2S layer decreases by about an order of magnitude. The same type of change occurs more slowly by simply exposing the Cu_2S - CdS layer to room air. Consequently, it is evident that the majority of the acceptors in this Cu_2S are oxygen atoms.

111. Ionic Mobility

Having established that the materials of this device are indeed semiconductors, it is clear that a p-n junction can result if two pieces of the proper carrier concentrations are placed in proper contact. Ideally, the energy diagram of the result is as shown in Figure 4.

The high mobility of the donor and acceptor ions in the solid considerably complicates the description of the device. That the ions must be mobile follows immediately from the manner in which Cu_2S is made. The chemical reaction is a double displacement with two copper ions replacing one cadmium

ion. This means that they must diffuse through the Cu_2S layer which is formed. Nominal reaction temperatures are 100°C and times are of the order of 1 minute to make 1 micron of Cu_2S. This means that 10^{20} to 10^{22} copper atoms diffuse into a 1 micron thick region in about 1 minute at 100°C. In silicon, 10^{18} phosphorus or boron atoms diffuse into a 1 micron region in about 1 hour at 800°C. This indicates a high difference in mobilities and further implies that the properties of silicon p-n junction and CdS - Cu_2S junction will be widely differing.

Analysis of the reaction kinetics in the solid allows the calculation of ionic diffusion constants. To begin, the chemical reaction takes place at the interface between the solution and solid CdS. In the solid, the processes are physical diffusions. On immersing CdS in the cuprous ion solution, a layer of Cu_2S is formed at the surface. The rate of formation is proportional to the amount of CdS present. Copper ions enter the solid and cadmium ions leave because of concentration gradients, the rate being governed by the diffusion equation, Mathematically, these are stated as:

$$\frac{d}{dt} C\ (x=o,t) = \alpha [C_o - C(x=o,t)]$$

$$D \frac{\partial^2}{\partial x^2} C(x,t) = \frac{\partial}{\partial t} C(x,t)$$

C = concentration of Cu_2S

C_o = bulk concentration of CdS

a = proportionality factor which is temperature dependent

D = copper ion diffusion constant

x = distance into solid

These equations can be solved, resulting in an expression which contains error functions with complex arguments. The general nature of the concentrations at any time is shown in Figure 5. Measurement of the concentration profile is difficult and uncertain for the cell geometry, It is easier to measure the total amount of Cu_2S formed as a function of time. For this, the solution of the equation is intergrated and approximated for long and short periods. For long times, the reaction is diffusion limited and the total mass has the familiar $t^{1/2}$ variation. For shorter times, the reaction is more de-

pendent on the surface reaction rate and the total mass varies at $t^{3/2}$. The exact expressions are:

$$M(t) = \frac{8C_o D^{5/2}}{\alpha \sqrt{\pi}} t^{3/2} \qquad \text{short times}$$

$$M(t) = \frac{2C_o D^{1/2}}{\sqrt{\pi}} t^{1/2} \qquad \text{long times}$$

By weighing the mass of Cu_2S formed as a function of time, the reaction limiting diffusion constant calculates to be

$$C(70°C) = 8 \times 10^{-10} \text{ cm}^2/\text{sec}$$

This agrees with the findings of Clarke[1].

By contrast, the diffusion constant for boron and phosphorus in silicon is of the order of 10^{-57} cm^2/sec at 100°C.

This high ionic mobility is also evidenced in the behavior of the rectifying junction under applied field. To look at this, let us first review the orthodox p-n junction, shown in Figure 6a. Here two materials have been brought into contact and to smooth out discontinuities, some electrons have left the n-region and entered the p-region, and some holes have gone from the p-region to the n-region. Uncompensated positively charged donor ions are in the n-region and uncompensated negatively charged acceptor ions are in the p-region.

This takes place in a distance equivalent to one diffusion length for the hole or electron. Typically, this will be in the region of 0.1 micron. The result is a dipole charge layer, positive in the n-region and negative in the p-region. A field is produced which tends to move positive charges from the n-region to the p-region. In the usual semiconductor, one now applies Boltzmann statistics, Poisson's equation and the continuity equation, arriving at the familiar diode equation relating the current and the potential difference across the junction.

$$I = I_o \left(e^{\frac{qV}{kT}} - 1\right)$$

In CdS and Cu_2S, however, the acceptor and donor ions are mobile. The field in the junction moves donors into the p-region and acceptors into the n-region. This continues until the field is balanced by concentration gradients in the usual manner. The

[1]Clarke, Raymond L. Journal of Applied Physics, Vol. 30, Number 7, pp. 957-960, July, 1959.

effect of this is to broaden the junction, and in fact, to produce a region of microscopic extent which is almost intrinsic as shown in Figure 6b. The geometry and properties of the junction will depend on the ionic mobilities. Obviously, if holes, electrons, and ions all had the same mobility, a junction would not exist.

The external manifestations of ion mobility are hysteresis in the dynamic I-V curve and an effect known as internal polarization. The first of these is seen when the I-V curve is traced at a finite speed, say 1 cycle per 10 minutes. Then the ascending and descending branches are separated, as in Figure 7. The second is seen by applying forward bias to the junction and allowing the current to reach a steady state. The applied field is removed and a meter placed across the cell terminal, Power will be delivered by the cell, on the order of microwatts/cm^2. The current produced will decay exponentially with time, time constantsbeing about 3 minutes. Referring to Figure 6b again, the origin of this effect is found in motion. of the ions. Forward bias places a potential difference across the junction which is negative on the n-side and positive on the p-side. This causes donor ions to move back to the n-region and acceptors to the p-region, and in the steady state concentration gradients again balance the internal and applied fields. When the field is removed, the ions return to their equilibrium positions, resulting in a current flow. The integrated current represents the total charge involved and the time constant of the discharge allows the calculation of an ion mobility. We assume the steady state field-applied condition to be two sheets of charge separated by the junction width, about 1 micron. Then the following relation holds:

$$\tau = \frac{W^2}{D}$$

τ = time constant = 3 minutes

W = junction width = 10^{-4} cm (by capacitance measurement)

D = diffusion constant

D then calculates to be about 5 x 10^{-11} cm^2/sec 'at 20°C, which is in good agreement with the value found from the chemical reaction kinetics.

The time constant for the polarization can be increased by widening the junction and decreasing the diffusion constant. The phenomenon in CdS known as persistent internal polarization is undoubtedly produced in a wide junction with low diffusion constant material.

It is also probable that the ion motion in the presence of light generated fields accounts for the photorectifier effect[2], and the non-linear addition of currents generated by differing colors of light. These are closely related to infrared quenching in photoconductors, and in fact, the whole process known as trapping would appear to be due to the junction and mobile ions.

IV. Microscopic Picture of Junction Formation

Having examined the properties of the materials in a CdS cell, it is now possible to follow the microscopic details of the cell forming process. A piece of crystalline CdS is immersed in the bath containing cuprous ions and a layer of Cu_2S from 0.1 to 1 micron thickness is formed. If oxygen is dissolved in the liquid, the layer can be doped at this time. Usually, the bath is around 100°C, the oxygen concentration is low, and the Cu_2S has low hole concentration. If the CdS has a low enough donor concentration ($10^{17}/cm^3$ or less), a p-n junction is formed immediately. This implies a background hole concentration in the Cu_2S of about $10^{17}/cm^3$. If the donor concentration is higher, there is no junction, and the cell has a linear 1-V relationship. Metal contacts are attached to the CdS and Cu_2S mechanically or by electroplating. A diode now forms either by heating in air or by simply remaining in room ambient. The exact behavior of the oxygen is shown in Figure 8. In part (a), the oxygen acceptors are in a complementary error function distribution and the maximum at the surface is less than the donor concentration, In (b), the acceptors have reached the level of the donors and a junction forms. This produces a field, which drives the acceptors into the n-region, widening the junction and reducing the field.

---

[2] Reynolds D. C., Green L. C., Antes L. L., Journal of Chemical Physics, Vol. 25, No, 6, pp. 1177-1179, December, 1956.

The surface acceptor concentration reaches a level determined by the atmospheric oxygen concentration. The junction width depends on this concentration, the donor concentration and the ionic diffusion constants. Heating the cell raises the diffusion constants and the junction widens, evidenced by a decrease in junction capacitance. Junction width will be essentially independent of the hole and electron lifetimes and diffusion length and will consequently not be depleted of charge. Hole-electron pairs generated in the junction will be separated, but the quantum yield will probably be significantly less than unity. Optimally, the junction will extend almost to the surface and look like (c).

Conclusion

A model of the CdS solar cell has been outlined in which the active elements are those things we know to exist (physically), that is, holes, electrons, acceptor and donor ions. The materials are semiconductors which follow Fermi Dirac statistics and conventional band theory. The unusual features of the device are seen to depend on highly mobile ions and in fact the high power conversion efficiency depends on them. This is consistent with the process by which the device is made, which also requires highly mobile ions. The similarity in properties between the CdS solar cell and the CdS photoconductor leads to the suspicion that traps are really mobile ions in junctions.

We wish to thank Dr. Robert Moss for his help in guiding physicists through the chemical jungle and Dr. Noel K. Pope for his invaluable guidance and advice in all aspects of the theory.

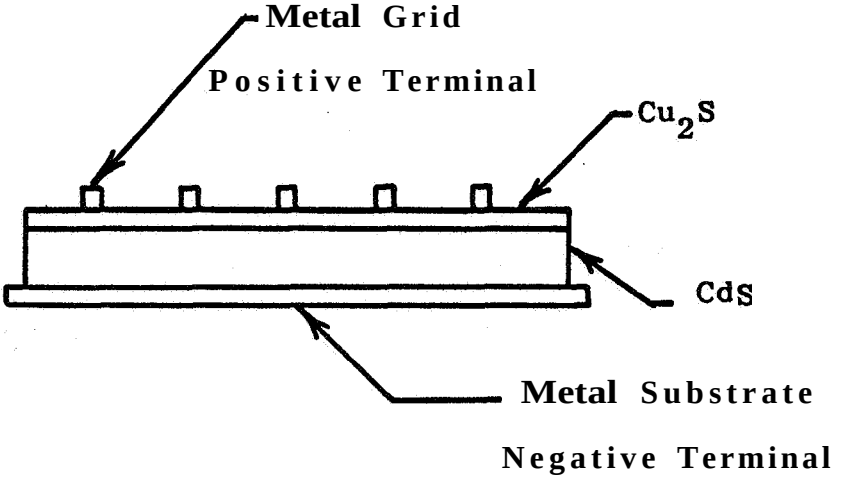

Fig. 1 Physical Schematic

Cross Section of CdS Solar Cell

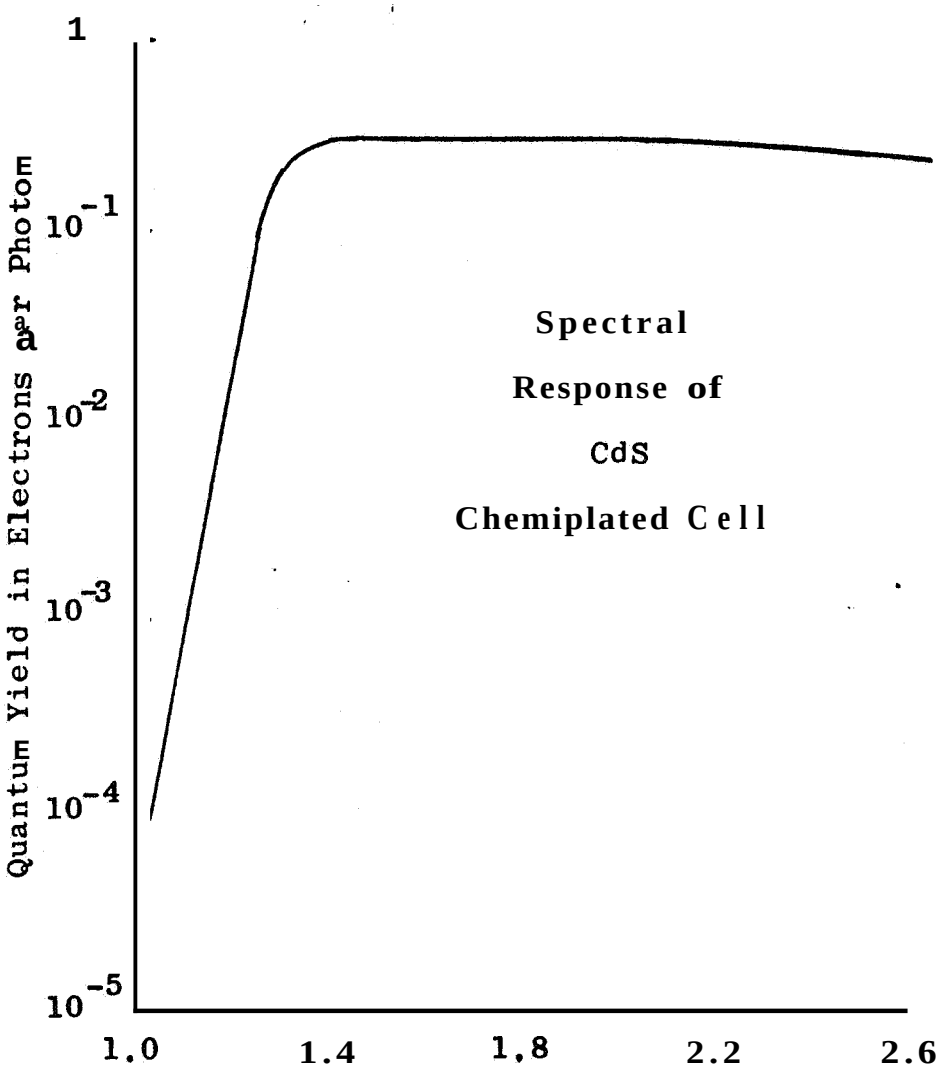

Fig. 2 Photon Energy in Electron Volts

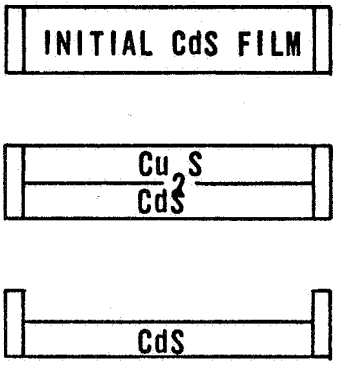

a/ CdS FILM

MEASURE R_a & α_a

b/ CdS - Cu_2S COMBINATION

MEASURE R_b & α_b

c/ CdS AFTER Cu_2S REMOVED BY KCN

MEASURE R_c, α_c

$$R(CdS) = R_c$$

$$R(Cu_2S) = \frac{R_b\, R(CdS)}{R(CdS) - R_b}$$

R = RESISTANCE

α = SEEBECK COEFFICIENT

$$\alpha(Cu_2S) = \alpha(CdS)\left(\frac{R(Cu_2S)}{R_c}\right) + \alpha_c\left(1 + \frac{R(Cu_2S)}{R_c}\right)$$

Fig. 3 MEASUREMENT OF ELECTRICAL PROPERTIES OF Cu_2S

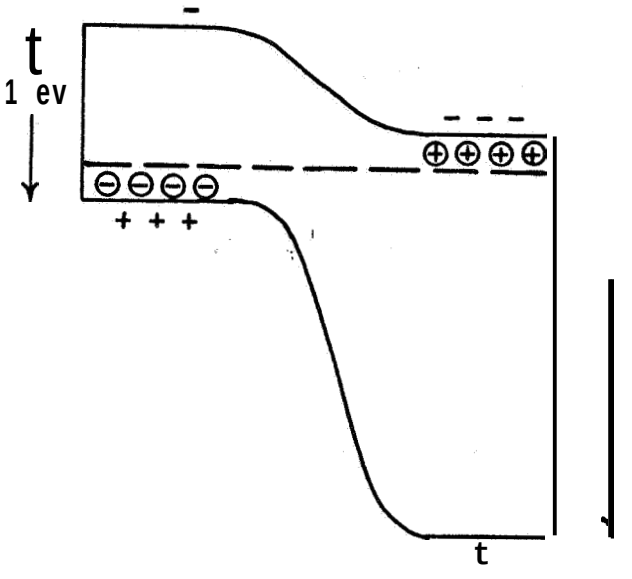

Fig. 4 ENERGY DIAGRAM FOR IDEAL HETEROJUNCTION OF CdS & Cu_2S

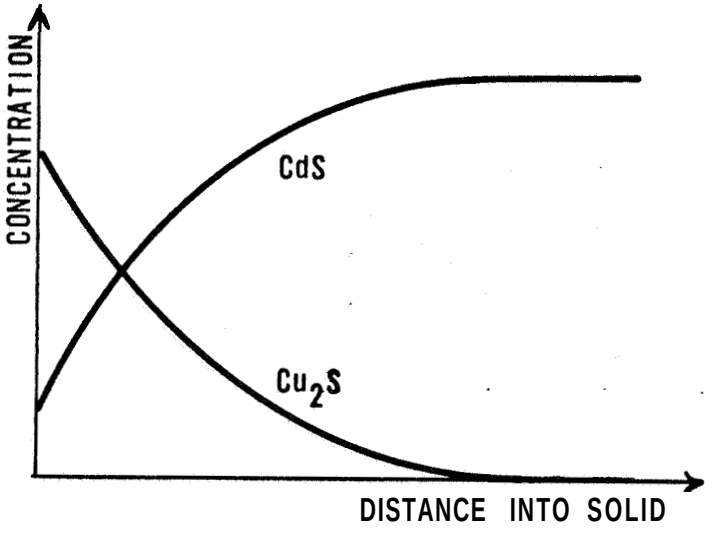

Fig. 5 SCHEMATIC DISTRIBUTION OF CdS & Cu_2S AFTER CHEMICAL REACTION

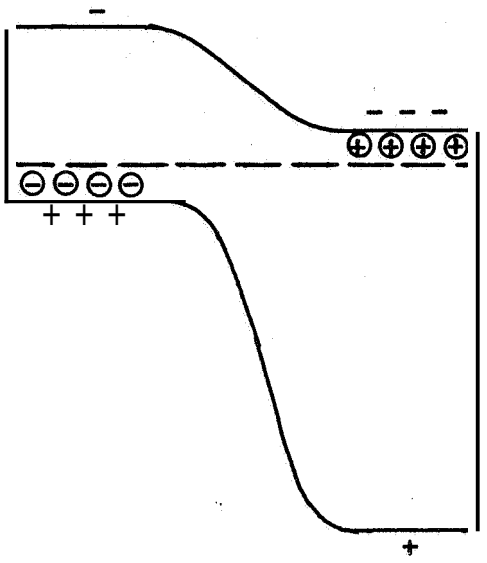

Fig. 6a ENERGY DIAGRAM FOR ORTHODOX p–n JUNCTION

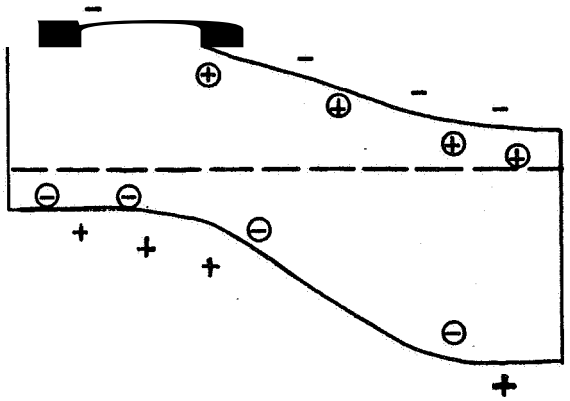

Fig. 6b ENERGY DIAGRAM FOR A p–n JUNCTION WITH MOBILE IONS

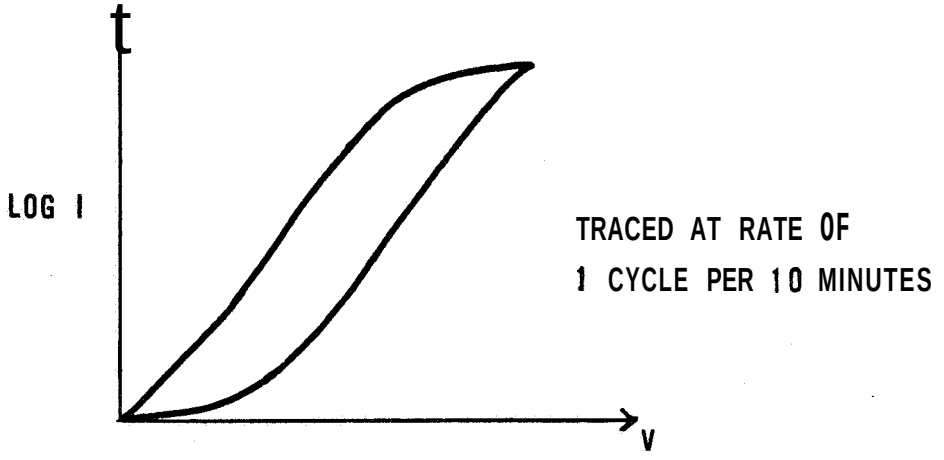

Fig. 7 DYNAMIC I–V CURVE FOR p–n JUNCTION WITH MOBILE IONS

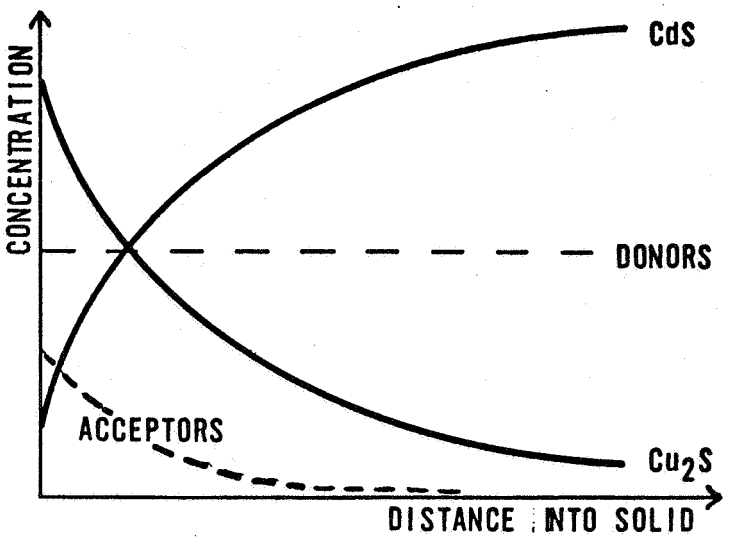

Fig. 8a IMPURITY DISTRIBUTION IN CdS CELL

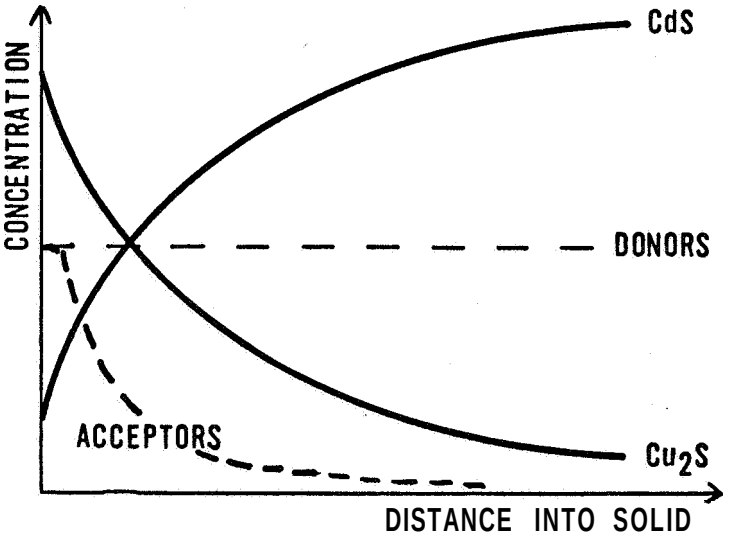

Fig. 8b IMPURITY DISTRIBUTION IN CdS CELL

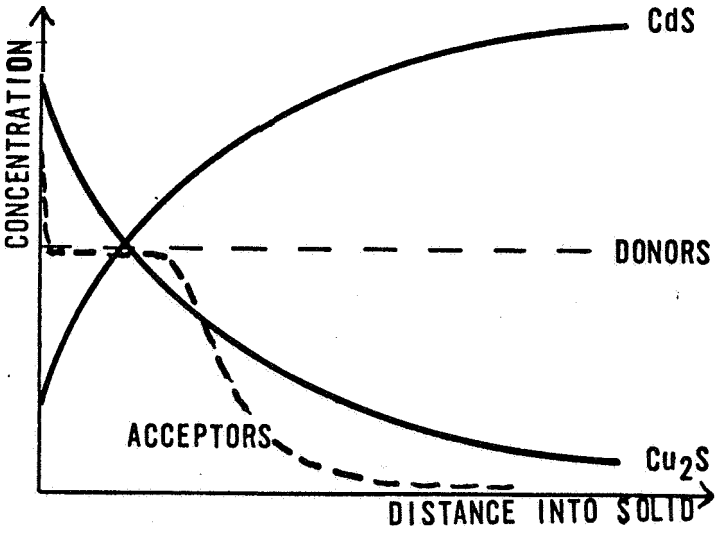

Fig 8c IMPURITY DISTRIBUTION IN CdS CELL

CONTRACT NAS3-8515
Final Reports

National Aeronautics and Space Administration
Washington, D. C. 20546
Attn: Arvin H. Smith/RNW (2)
H. B. Finger/RP
Mil1ie Ruda/AFSS-LD

National Aeronautics and Space Administration
Scientific and Technical Information Facility
P. O. Box 33
College Park, Maryland 20740
Attn: Acquisitions Branch (SQT-34054) (2+1 repro.)

National Aeronautics and Space Administration
Goddard Space Flight Center
Greenbelt, Maryland 20771
Attn: W. R. Cherry
M. Schach
B. Mermelstein, Code 672
J. W. Callaghan, Code 621
Librarian
P. H. Fang, Code 633

National Aeronautics and Space Administration
Lewis Research Center
21000 Brookpark Road
Cleveland, Ohio 44135
Attn: John E. Dilley, MS 500-309
B. Lubarsky, MS 500-201
A. F. Forestieri, MS 500-201
R. L. Cummings, MS 500-201
C. K. Swartz, MS 500-201 (3+1 repro.)
N. D. Sanders, MS 302-1
A. E. Potter, MS 302-1 (3)
V. F. Hlavin, MS 3-14 (Final Report Only)
George Mandel, MS 5-1 (2)
Report Control Office, MS 5-5
Technology Utilization Office, MS 3-19

National Aeronautics and Space Administration
Langley Research Center
Langley Station
Hampton, Virginia 23365
Attn: W. C. Hulton
E, Rind

National Aeronautics and Space Administration
Electronic Research Center
Power Conditioning & Distribution Lab.
575 Technology Square
Cambridge, Massachusetts 02139

Jet Propulsion Laboratory
4800 Oak Grove Drive
Pasadena, California 91103
Attn: John V. Goldsmith
Don W. Ritchie

Institute for Defense Analysis
400 Army-Navy Drive
Arlington, Virginia 22202
Attn: R. Hamilton

Advanced Research Projects Agency
Department of Defense, Pentagon
Washington, D. C. 20546
Attn: Dr. C. Yost

Naval Research Laboratory
Department of the Navy
Washington, D. C. 20546
Attn: E. Broncato, Code 6464
M. Wotaw, Code 5170
Dr. V. Linnenbom, Code 7450
Dr. C. Klick, Code 6440

Commanding Officer
U. S. Army Electronics R&D Labs
Fort Monmouth, New Jersey 07703
Attn: Power Sources Division SELRA/PS

Air Force Cambridge Research Center
Air Research and Development Command
United States Air Force
Laurence G. Hanscom Field
Bedford, Massachusetts 01731
Attn: Col. G. de Giacomo

Air Force Ballistic Missile Division
Air Force Unit Post Office
Los Angeles, California 90045
Attn: Col. L. Norman, SSEM
Lt. Col. G. Austin, SSZAS
Lt. Col. A. Bush, SSZME
Capt. A. Johnson, SSZDT
Capt. W. Hoover, SSTRE

Office of the Chief of Engineers
Technical Development Branch
Washington, D. C. 20546
Attn: James E. Melcoln/ENGMC-ED

Aeronautical Research Laboratories
Office of Aerospace Research, USAF
Wright-Patterson Air Force Base
Dayton, Ohio 45433
Attn: Mr, D. C. Reynoles, ARX
Chief, Solid State Physics,
Research Lab.

Aeronautical Systems Division
Air Force Systems Command
United States Air Force
Wright-Patterson Air Force Base, Ohio 45433
Attn: P. R. Betheand
Mrs, E. Tarrants/WWRNEM-1

Flight Vehicle Power Branch
Air Force Aero Propulsion Laboratory
Wright-Patterson Air Force Base, Ohio 45433
Attn: Joe Wise/Code APIP-2

Flight Accessories Aeronautics Systems Division
Wright-Patterson Air Force Base
Dayton, Ohio 45433
Attn: James L. Matice, ASRCM-22

Aerospace Corporation
P. 0. Box 95085
Los Angeles, California 90045
Attn: Dr. G. Hove
Dr, F. Mozer
V. J. Porfune
Dr. I, Spiro
Technical Library Documents Group

Battelle Memorial Institute
505 King Avenue
Columbus, Ohio 43201
Attn: L. W. Aukerman
R, E. Bowman
T. Shielladay

Bell and Howell Research Center
360 Sierre Madre Villa
Pasadena, California 91109
Attn: Alan G. Richards

Bell Telephone Laboratories, Incorporated
Murray Hill, New Jersey 07971
Attn: W. L. Brown
U. B. Thomas

Clevite Corporation
Electronic Research Division
540 Wast 105th Street
Cleveland, Ohio 44108
Attn: Fred A. Shirland
Dr. Hans Jaffe

The Eagle-Picher Company
Chemical and Material Division
Miami Research Laboratories
200 Ninth Avenue, N.E.
Miami, Oklahoma 74354
Attn: John R. Musgrave

Energy Conversion, Incorporated
336 Main Street
Cambridge, Massachusetts 02142
Attn: G. J. McCaul

General Electric Company
Electric Components Division
316 East Ninth Street
Owensboro, Kentucky 42301
Attn: F. D. Dyer, Jr.

Heliotek Corporation
12500 Gladstone Avenue
Sylmar, California 91342
Attn: Eugene Ralph

Hughes Aircraft Company
Aerospace Group, R&D Division
Culver City, California
Attn: C. A. Escoffery

International Rectifier Corporation
239 Kansas Street
El Segundo, California 90245
Attn: Irwin Rubin

Leesona Moos Laboratories
90-28 VanWyck Expressway
Jamaica, New York 11021
Attn: Stanley Wallack

Lockheed Missile and Space Division
3251 Hanover Street
Palo Alto, California 94304
Attn: D. Marks, Dept. 5230

Material Research Corporation
Orangeburg, New York 10962
Attn: Vernon E. Adler

National Cash Register Company
Physical Research Department
Dayton, Ohio 45409
Attn: R. R. Chamberlin

North American Aviation, Incorporated
Autonetics Division
Anaheim, California 92803
Attn: R. R. August

Perkin-Elmer Company
Optical Coating Section
Norwalk, Connecticut 06845
Attn: Jim Peardsley

Philco Corporation
Blue Bell, Pennsylvania 19422
Attn: A. E. Mace

Physics Technology Laboratories, Inc.
7841 El Cajon Boulevard
La Masa, California 92041
Attn: W. E. Richards

RCA Laboratories
Radio Corporation of America
Princeton, New Jersey 08540
Attn: P. Rappaport
M. Wolf
M. L. Topfer

Ryan Aeronautical Company
Lindbergh Field
San Diego, California 92112
Attn: K. D. Hawkins

Sandia Corporation
Albuquerque, New Mexico 87116
Attn: F. Smits

Sylvania Electronic Products, Incorporated
Electron Tube Division
Emporium, Pennsylvania 15834
Attn: Georgiana Larrabee, Librarian

Tyco Laboratories, Incorporated
Bear Hill
Waltham, Massachusetts 02154
Attn: A. I. Mlavsky

Union Carbide Corporation
Parma Research Center
Technical Information Services
P. O. Box 6116
Cleveland, Ohio 44101

Solid-State Electronics Laboratory
Stanford Electronics Laboratories
Stanford University
Stanford, California 94305
Attn: Professor G. L. Pearson

Westinghouse Electric Corporation
Research and Development Laboratories
Churchill Borough, Pennsylvania 15235
Attn: H. G. Chang

Westinghouse Electric Corporation
Semiconductor Division
Youngwood, Pennsylvania 15697
Attn: Don Gunther

Massachusetts Institute of Technology
Security Records Office
Room 14-0641
Cambridge, Massachusetts 02139

G. T. Schjeldahl Company
Northfield, Minnesota 55057
Attn: Don Roiseland

The Boeing Company
P. O. Box 3707
Seattle, Washington 98124

TRW Systems
Electric Power Laboratory
One Space Park
Redonao Beach, California
Attention: W. Luft